Received: 5 April 2018 | Revised: 3 September 2018 | Accepted: 17 September 2018

DOI: 10.1111/cmi.12976

RESEARCH ARTICLE

WILEY

Host membrane glycosphingolipids and lipid microdomains facilitate *Histoplasma capsulatum* internalisation by macrophages

Allan J. Guimarães[1,2] | Mariana Duarte de Cerqueira[3] | Daniel Zamith-Miranda[3] | Pablo H. Lopez[4†] | Marcio L. Rodrigues[3,5] | Bruno Pontes[6] | Nathan B. Viana[6,7] | Carlos M. DeLeon-Rodriguez[8] | Diego Conrado Pereira Rossi[8] | Arturo Casadevall[8] | Andre M.O. Gomes[9] | Luis R. Martinez[10] | Ronald L. Schnaar[4] | Joshua D. Nosanchuk[2*] | Leonardo Nimrichter[3*]

[1] Department of Microbiology and Parasitology, Biomedical Institute, Fluminense Federal University, Rio de Janeiro, Brazil

[2] Departments of Medicine (Division of Infectious Diseases) and Microbiology and Immunology, Albert Einstein College of Medicine, Bronx, New York

[3] Department of General Microbiology, Microbiology Institute, Federal University of Rio de Janeiro, Rio de Janeiro, Brazil

[4] Department of Pharmacology and Molecular Sciences, Johns Hopkins University School of Medicine, Baltimore, Maryland

[5] Instituto Carlos Chagas, Fundação Oswaldo Cruz (Fiocruz), Curitiba, Brazil

[6] LPO-COPEA, Institute of Biomedical Sciences, Federal University of Rio de Janeiro, Rio de Janeiro, Brazil

[7] LPO-COPEA, Institute of Physics, Federal University of Rio de Janeiro, Rio de Janeiro, Brazil

[8] Department of Molecular Microbiology and Immunology, Johns Hopkins Bloomberg School of Public Health, Baltimore, Maryland

[9] Program of Structural Biology, Institute of Medical Biochemistry Leopoldo de Meis and National Institute of Science and Technology of Structural Biology and Bioimaging, Federal University of Rio de Janeiro, Rio de Janeiro, Brazil

[10] Biological Sciences, The University of Texas at El Paso, El Paso, Texas

Correspondence
Leonardo Nimrichter, Institute of Microbiology Professor Paulo de Góes, Federal University of Rio de Janeiro, Health Sciences Center, block I. 21941590, Rio de Janeiro, Brazil.
Email: nimrichter@micro.ufrj.br

Joshua D. Nosanchuk, Departments of Medicine (Division of Infectious Diseases) and Microbiology and Immunology, Albert Einstein College of Medicine, 1300 Morris Park Ave., Bronx, NY 10461.
Email: josh.nosanchuk@einstein.yu.edu

Present Address
Pablo H. Lopez, Instituto de Investigación Médica Mercedes y Martin Ferreyra (INIMEC–CONICET) and Facultad de Psicología, Universidad Nacional de Córdoba, Córdoba, 5000, Argentina.

Funding information
A.J.G and J.D.N., Grant/Award Number: NIH AI056070-01A2 and the Center for AIDS Research; A.J.G., L.N., M.L.R., B.P., N.BV. and D.Z-M., Grant/Award Number: Conselho Nacional de Desenvolvimento Tecnológico;

Abstract

Recognition and internalisation of intracellular pathogens by host cells is a multifactorial process, involving both stable and transient interactions. The plasticity of the host cell plasma membrane is fundamental in this infectious process. Here, the participation of macrophage lipid microdomains during adhesion and internalisation of the fungal pathogen *Histoplasma capsulatum* (Hc) was investigated. An increase in membrane lateral organisation, which is a characteristic of lipid microdomains, was observed during the first steps of Hc–macrophage interaction. Cholesterol enrichment in macrophage membranes around Hc contact regions and reduced levels of Hc–macrophage association after cholesterol removal also suggested the participation of lipid microdomains during Hc–macrophage interaction. Using optical tweezers to study cell-to-cell interactions, we showed that cholesterol depletion increased the time required for Hc adhesion. Additionally, fungal internalisation was significantly reduced under these conditions. Moreover, macrophages treated with the ceramide-glucosyltransferase inhibitor (P4r) and macrophages with altered ganglioside synthesis (from *B4galnt1*$^{-/-}$ mice) showed a deficient ability to interact with Hc. Coincubation of oligo-GM1 and treatment with Cholera toxin Subunit B, which recognises the ganglioside GM1, also

Allan J. Guimarães and Mariana Duarte de Cerqueira share first authorship on the manuscript.
*Leonardo Nimrichter and Joshua D. Nosanchuk share senior authorship on the manuscript.

LN, Grant/Award Number: Fulbright (Visiting Scientist/Visiting Professor S; LN and AJG, Grant/Award Number: Interhemispheric Research Training Grant in Infect; RS, Grant/Award Number: Mutant mice and ganglioside oligosaccharides were; National Institutes of Health, Grant/Award Number: NS037096; CAPES-Fulbright (Visiting Scientist/Visiting Professor Scholar Program); Conselho Nacional de Desenvolvimento Tecnológico (CNPq, Brazil) and Fundação Carlos Chagas Filho de Amparo à Pesquisa do Estado do Rio de Janeiro (FAPERJ, Brazil); Center for AIDS Research at the Albert Einstein College of Medicine and Montefiore Medical Center, Grant/Award Numbers: NIH AI-51519 and NIH AI056070-01A2; Interhemispheric Research Training Grant in Infectious Diseases, Fogarty International Center, Grant/Award Number: NIH D43-TW007129

reduced Hc association. Although purified GM1 did not alter Hc binding, treatment with P4 significantly increased the time required for Hc binding to macrophages. The content of CD18 was displaced from lipid microdomains in *B4galnt1*$^{-/-}$ macrophages. In addition, macrophages with reduced CD18 expression (CD18^{low}) were associated with Hc at levels similar to wild-type cells. Finally, CD11b and CD18 colocalised with GM1 during Hc–macrophage interaction. Our results indicate that lipid rafts and particularly complex gangliosides that reside in lipid rafts stabilise Hc–macrophage adhesion and mediate efficient internalisation during histoplasmosis.

KEYWORDS

glycosphingolipids, *Histoplasma capsulatum*, lipid rafts, macrophages

1 | INTRODUCTION

Glycosphingolipids (GSLs) are components of plasma membranes of virtually all eukaryotic cells (Hakomori, 2003). Besides their complex roles as components of biological membranes, they also participate in immunoregulatory processes, including modulation of cytokine production and lymphoproliferative responses (Das et al., 2008; Vieira et al., 2008). In concert with sterols, GSLs laterally associate with other molecules including pathogen receptors and GPI-anchored proteins within special regions of membranes called lipid microdomains (Brown & London, 2000). Association of pathogen receptors with lipid microdomains implies that these regions are involved in host–pathogen interactions (Cuschieri, Billigren, & Maier, 2006; Grassme et al., 2003; Triantafilou, Miyake, Golenbock, & Triantafilou, 2002; Triantafilou & Triantafilou, 2003). In fact, viruses, bacteria, protozoa, fungi, and even prions exploit lipid microdomains to invade phagocytic and nonphagocytic host cells (Goluszko, Popov, Wen, Jones, & Yallampalli, 2008; Kalischuk, Inglis, & Buret, 2009; Lafont & van der Goot, 2005; Maza, Straus, Toledo, Takahashi, & Suzuki, 2008; Murphy et al., 2006).

Histoplasma capsulatum (Hc) is the etiologic agent of histoplasmosis, one of the most common invasive fungal pulmonary diseases (Cano & Hajjeh, 2001; Pfaller & Diekema, 2010). This organism is a classical intracellular pathogen that replicates within macrophages and suborns the reticuloendothelial system to disseminate (reviewed by Kauffman, 2009). The infection is usually asymptomatic in immunocompetent individuals, although several thousand admissions for histoplasmosis occur annually in the United States (Kauffman, 2009). Disseminated histoplasmosis is more common in immunocompromised patients, especially in individuals with AIDS (Kauffman, 2009; Rodrigues et al., 2008).

Hc interacts primarily with CR3 at the macrophage (Mφ) surface (Bullock & Wright, 1987) through a 60-kDa heat shock protein (HSP60) expressed at the fungal cell wall (Long, Gomez, Morris, & Newman, 2003). CD18, the β subunit of the $\alpha_m\beta_2$ integrin CR3, appears to be the site of CR3 to which Hc binds, although antibodies to CD11b also decrease the association levels (Lin, Huang, Hung, Wu, & Wu-Hsieh, 2010; Long et al., 2003). Internalisation of nonopsonised fungi occurs via CR3 and typically results in fungal survival inside resident Mφs (Lin et al., 2010; Newman, 1999, Strasser et al., 1999, Shi et al., 2008).

Here, we investigated the role of GSL and lipid microdomains during initial steps of interaction between Hc and murine macrophages (Mφs). Two-photon excitation confocal fluorescence microscopy of live cells was used to show in real time the formation of organised lipid domains at the site of interaction of Hc with the Mφs membranes. We used cellular systems that included cultured or bone marrow-derived Mφs (BMDMs) from mice genetically deficient in the synthesis of complex sialylated GSL (including II^3-*N*-acetylneuraminosylgangliotetraosylceramide or GM1), CD11b, and CD18, with the use of sterol- and GSL-specific reagents and an optical tweezers (OTs)-based experimental model to evaluate fungus–host cell affinity. Using OTs, we estimated the time required for adhesion between Hc and Mφs, with a focus on the participation of lipid microdomain components. Our results demonstrated that depletion of cholesterol interferes with Hc adhesion kinetics and internalisation. The participation of CD18 and CD11b during Hc association was also compared using genetically deficient mice. In addition, GSL participated in the initial steps of Mφ interaction and infection by a fungal pathogen. Interfering with microdomain assembly and protein recruitment could potentially affect macrophage responses, with direct impact on disease development or progression.

2 | RESULTS

2.1 | Hc contact with the Mφ plasma membrane induces formation of lipid microdomains at contact sites

Lipid microdomains present a characteristic lateral organisation that can be accessed by environment-sensitive fluorescent molecules (Sanchez, Tricerri, Gunther, & Gratton, 2007). Using Laurdan fluorescence microscopy, one can obtain a map of the spatial distribution of lipid phases along the cell membranes. In a time-lapse microscopy experiment, these maps are representative of the dynamics of

formation and localisation of lipid domains in the cell membrane. With this approach, we obtained Laurdan General Polarisation or GP images during the interaction between Hc and Mφs in real time. Laurdan GP has been measured before to characterise laterally organised lipid domains in synthetic and cellular membranes including Mφs membranes (Gaus et al., 2003). To investigate if lipid microdomains are involved in Hc binding to the surface of Mφs, we incubated these cells with Laurdan, which partitions into the lipid bilayer. Hc–Rhodamine (Hc-Rho) yeasts were added over the Laurdan-loaded Mφs. The interaction was imaged in a two-photon excitation microscope by a time-lapse sequence of images acquired in real-time during contact and internalisation of Hc cells by the Mφs. A time-lapse series of 90 images was acquired (one frame per second). Figure 1a–c shows, respectively, the Laurdan intensity images at 440, 490, and Hc fluorescence at frame number 15. Figure 1d–f shows merges of Channels 1, 2, and 4, at Frames 15, 45, and 75 as representatives of initial, middle, and advanced stages of the interaction process. Using the intensity images in Channels 1 and 2, the Laurdan GP image sequence can be calculated as described in Experimental Procedures, and changes in lipid organisation at the macrophage membrane level can be followed during the interaction process. Figure 1g–i shows the respective GP images of Frames 15, 45, and 75, merged with the correspondent Hc fluorescence images. The average change in membrane organisation as a function of time is plotted in Figure 1j. The purple line represents changes in average GP values of all Mφs membranes imaged, and the average GP values for specific Hc contact sites are plotted in green (Figure 1j). The interaction time sequence can be divided in three parts of 30 s each. The first 30 s show that during the first steps of contact of Hc with macrophages, the GP values on the contact area were higher than the Mφs membranes average (Hc-contact areas mean = 0.45, *SD* = 0.01; Mφs mean = 0.38, *SD* = 0.02, $t(40) = -12.9$, $P = 7.67 \times 10^{-16}$, significantly different). As the process continues, the values of the averages become very close. Finally, in the last 30 s, there is almost no difference between Hc-contact areas and Mφs, with macrophage membranes average showing a slightly higher average GP value (Hc-contact areas mean = 0.41, *SD* = 0.017; Mφs mean = 0.42, *SD* = 0.009, $t(38) = 3.91$, $P = 0.0004$, significantly different). Notably, the average GP of macrophages increased during internalisation of Hc (mean of first 10 frames = 0.38, *SD* = 0.006; last 10 frames mean = 0.43 and *SD* = 0.004; $t(16) = -21.6$, $P = 2.88 \times 10^{-13}$, significantly different; Figure 1 and more details in Table S1).

2.2 | Disruption of lipid domains with m-β-CD decreases Hc association with Mφs

Filipin staining of Hc adhered to J774.16 Mφs revealed enrichment of sterols on the adhesion area (Figure 2a–d), indicating that cholesterol within microdomains could be involved in Hc-Mφs recognition. Treatment of J774.16 Mφs with methyl-β-cyclodextrin (m-β-CD) removes sterols from cell membranes causing lipid microdomain disruption. To test this hypothesis, we then measured the percentage of Hc-Mφs association, which includes the total of Mφs where Hc are adhered or internalised, in the presence and absence of m-β-CD. Incubation of Mφs with m-β-CD decreased their association with Hc in a dose-dependent fashion (Figure 2d,e), especially at early time points (15 min, Figure 2d). Although opsonisation with a monoclonal antibody (mAb) to heat shock protein 60 (HSP60; mAb 7B6) did not change the association level in control Mφs, it partially reversed the inhibition caused by previous m-β-CD treatment. A second mAb against a different surface antigen (M antigen, mAb 6F12) had a similar effect (Figure 2d,e). When the incubation period was increased to 45 min, a similar tendency was observed, but no statistical differences were detected (Figure 2e). Overall, the association of opsonised yeast was abruptly decreased by m-β-CD treatment after 15 min of interaction, with a significant reversion in the magnitude of effect over time suggesting that remodelling of microdomains is important during the initial steps of fungi–phagocyte interaction.

Mφ metabolic integrity was assessed using methylthiazolyldiphenyl-tetrazolium 1 hr after treatment with m-β-CD (0 to 20 mM). At the highest dose, a trend towards lower metabolic activity was observed, as previously described in several models (Kainu, Hermansson, & Somerharju, 2010; Piel et al., 2007). However, using a Trypan Blue assay, the cells displayed approximately 100% of membrane integrity in all conditions tested (data not shown).

2.3 | Fungal adhesion to Mφs is dependent on the integrity of lipid rafts

The results above indicate that lipid raft disruption might interfere with the kinetics of Hc-Mφs association. Using OTs, we were able to access this kinetics by measuring the characteristic time (τ) required for adhesion of Hc to Mφs, the step that precedes fungal phagocytosis. A plot of the relative adhesion as a function of time revealed that the number of positive adhesions between Hc and J774.16 Mφs increased with time in all experimental conditions (Figure 3). Treatment with 10-mM m-β-CD slowed the rate of yeast–Mφ stable adhesion nearly threefold. Whereas opsonisation increased the rate of association to both control and m-β-CD-treated Mφs, raft disruption again slowed the relative rate of stable adhesion, in this case approximately fourfold. The characteristic time values obtained by OTs are in agreement with the association results.

2.4 | Treatment with m-β-CD also reduces the capacity of Mφs to phagocytose Hc

Cholesterol depletion influences adhesion during the first minutes of Mφs-Hc interaction. We then investigated whether treatment with m-β-CD also impacts Hc internalisation by J774.16 Mφs after 45-min interaction (Figure 4a and Table S2). When experiments were performed using nonopsonised fungi and control Mφs, we observed that 71% of associated Hc were internalised in 45 min. For these analyses, only the Mφs containing at least one Hc attached were considered for comparison between adhered and internalised yeasts. Furthermore, because there was no difference between GFP-Hc and NHS-Rho-Hc association to Mφs (data not shown), NHS-Rho did not impair Hc recognition by Mφs. Treatment with 5- and 10-mM m-β-CD reduced the internalisation of Hc by treated Mφs by nearly 20%. Treatment with

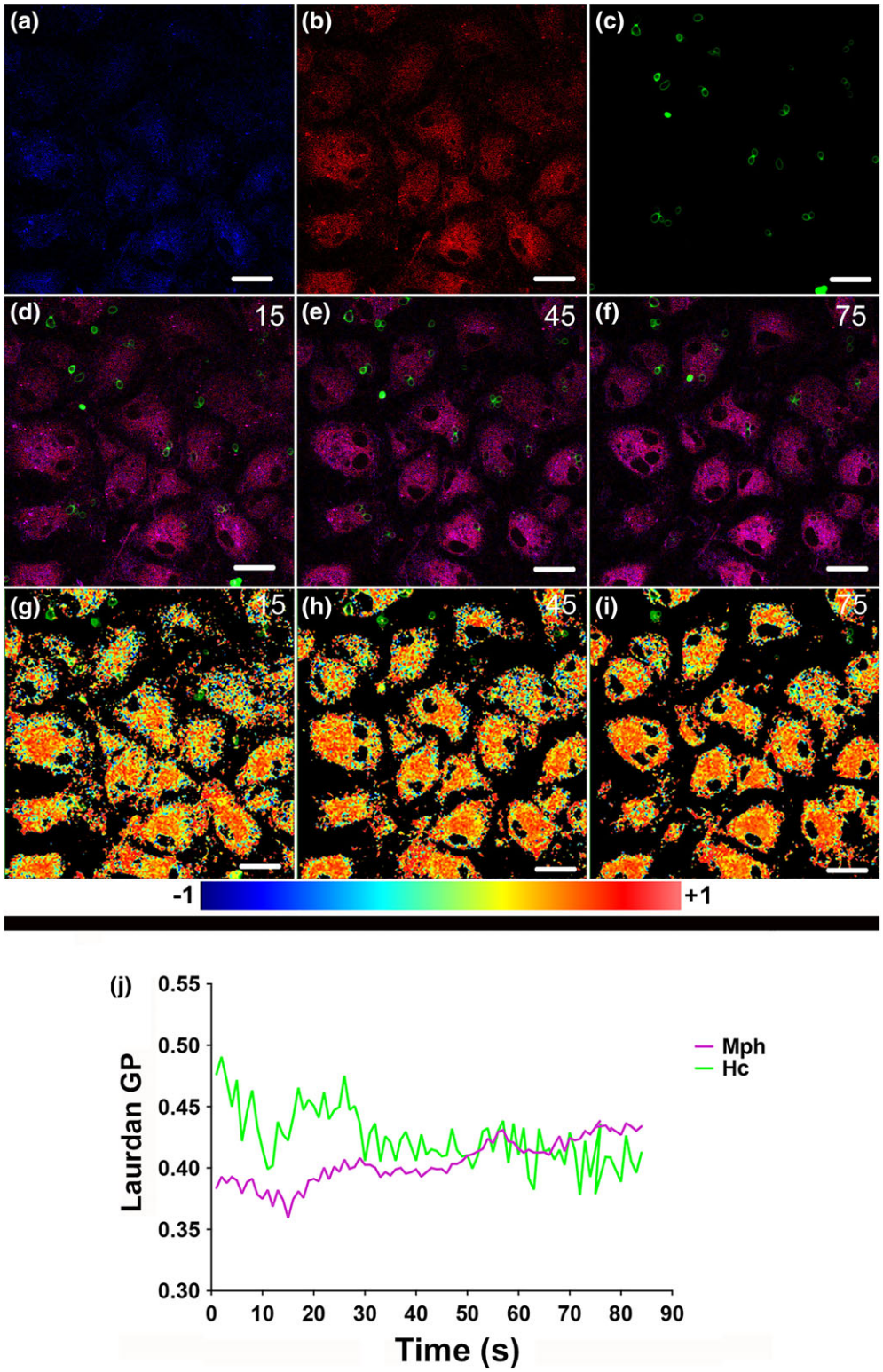

FIGURE 1 Hc yeast cells induce dynamic changes of lateral organisation in Mφ membranes. Hc-Rho yeast cells were plated onto bone marrow-derived murine Mφs previously stained with Laurdan. (a) Channel 1: 440 nm, arbitrarily coloured blue, (b) Channel 2: 490 nm, arbitrarily coloured red, and (c) Channel 3: 595 nm, arbitrarily coloured green depict the first frame displaying the interaction of Hc yeasts and Mφ. Merge images of the three channels are shown in three distinct time frames ([d–f] 15, 45, and 90 s of interaction). GP images at the same time frames merged with Hc-Rho images showing the increase in lateral organisation over the time of interaction (g–i). GP values over this time course are depicted in panel j where the purple line represents average GP values of Mφ membranes and the green line represents the average GP specifically at the Hc-Mφ contact regions. Statistics were performed for (i) all frames, (ii) the first and last 10 min, and (iii) the three sets of frames (30, 60, and 90). Representative of three independent experiments, differences considered significant by unpaired *t* test. For all analyses $P < 0.001$ (see details in Table S2). Bar, 10 μm

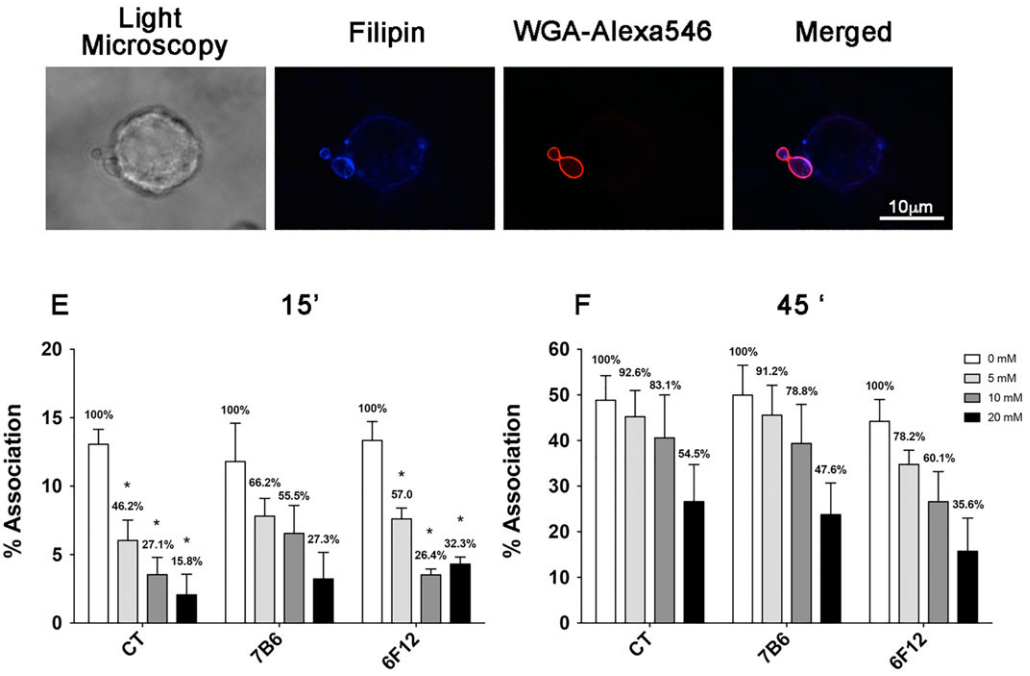

FIGURE 2 Importance of sterols in the Hc association with macrophages and effect of m-β-CD treatment on the association with Hc. (a) Light microscopy of Mφ-Hc interaction. (b,c) Filipin staining of cholesterol in J774.16 Mφ membranes and WGA-Alexa546 in Hc. (d) Merged images denoting the colocalisation of filipin staining and WGA-Alexa546-Hc. Bar, 10 μm. (e) GFP-Hc yeast cells with or without opsonisation with antibodies to HSP60 (mAb 7B6) or to M antigen (mAb 6F12) were incubated for 15 or (f) 45 min with J774.16 Mφs pretreated with different concentrations of m-β-CD. Samples were analysed by flow cytometry. Bars show the percentage of yeast-associated Mφs over the total number of Mφs analysed. The numbers on the bars indicate the total infected Mφs in each system followed by the percentage determined in the setting of infection compared to controls (considered as 100%). The results shown are the average of three independent experiments. Each individual system showed statistical significance ($P < 0.0001$) in comparison with its appropriate control

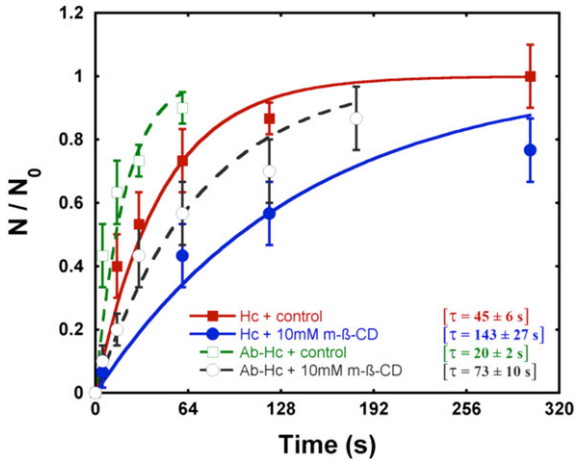

FIGURE 3 Optical tweezers-based determination of Hc adhesion to Mφs. Treatment of J774.16 Mφs with 10-mM m-β-CD (blue) results in a decreased during the adhesion kinetic, in comparison with systems using control Mφs (red). Antibody-treatment of Hc followed by interaction with control (green) or m-β-CD-treated (grey) Mφs enhances adhesion in comparison with systems where opsonisation was not performed. The data shown are averages of results from three independent experiments. The error bars were determined as half the difference between the maximum and minimum values for each interval in 30 events performed in three distinct samples. The characteristic time (τ) required for adhesion is also shown

20-mM m-β-CD resulted in almost complete abrogation of internalisation. Inhibition of phagocytosis was overcome by opsonisation of yeasts with antibodies to HSP60, except at the highest concentration of m-β-CD, in which the inhibitory conditions were only slightly reduced by opsonisation. This observation is in agreement with a possible impairment of interaction through FcγR or an alternative mechanism of association of yeast by a low affinity nonraft receptor. In combination with the observation that only the treatment with 20-mM m-β-CD efficiently reduced the association index at 45 min (Figure 2), these data suggest that cholesterol depletion impacts both adhesion and internalisation of Hc by Mφs. Because m-β-CD efficiently extracts proteins from cell surfaces (Ilangumaran & Hoessli, 1998), we next tested whether CR3 components were normally detected in m-β-CD-treated cells. The membrane levels of CD18 and CD11b, which are well-characterised receptors for Hc (Long et al., 2003) were not altered by m-β-CD treatment (Figure 4b).

2.5 | Inhibition of GSL synthesis by Mφs reduces Hc association

We then explored the role of GSL, another class of lipids enriched in microdomains, during Hc association by using J774.16 Mφs treated with P4 ((1*R*,2*R*) 1-phenyl-2-palmitoylamino-3-pyrrolidino-1-propanol), a specific inhibitor of GSL biosynthesis (Nicholson, Quinn, Kellett, & Warr, 1999). Mφs were treated with P4r (active isomer) or P4s (the 1*S*,2*S* inactive isomer) as a control for 3 days. Under the conditions used in our experiments, P4r treatment resulted in approximately 60% inhibition of ganglioside synthesis in BMDMs (Figure S1). Treatment also minimally reduced sphingomyelin and ceramide (approximately 10% and 14%, respectively), when compared with the

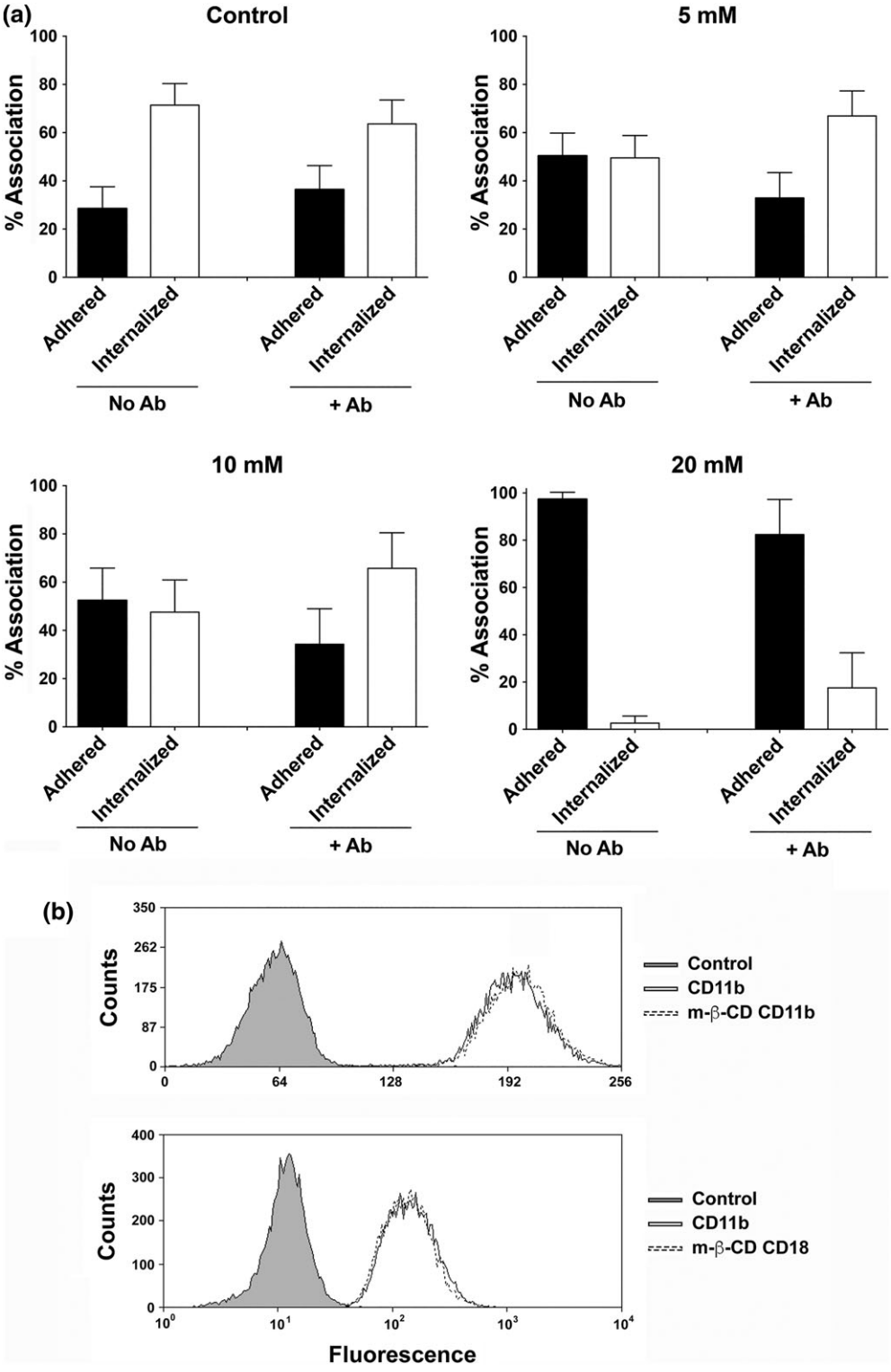

FIGURE 4 Disruption of membrane rafts by m-*β*-CD decreases adhesion and internalisation of Hc yeasts. (a) J774.16 Mφs were treated, or not with 5, 10, or 20 mM of m-*β*-CD and then incubated with nonopsonized (left panels) or anti-Hsp60 mAb opsonized (right panels) yeast previously labelled with NHS-Rho. After 45 min of interaction, Uvitex 2B was added to stain extracellular fungi. Percentages of adherent and internalised yeasts are only for Mφs associated with Hc. The effect on sterol depletion by m-*β*-CD treatment was overcome by yeast opsonisation at concentrations of 5 and 10 mM and partially reversed at 20-mM m-*β*-CD. (B) Mφs treated with 10 mM of m-*β*-CD were also labelled with anti-CD11b or CD18 to confirm the levels of CR3 on the cell surface, and no changes were detected. The experiments were performed three different times with similar results. Statistical analyses of these data are shown in Table S2

inactive control P4s (Figure S2). In addition, P4r treatment reduced the Mφ-Hc association by 30% compared with P4s-treated cells ($P < 0.05$), suggesting the involvement of gangliosides during Hc infection of Mφs (Figure 5a). Corroborating with these data, the characteristic time (τ) required for adhesion of Hc yeasts was significantly increased in P4r-treated Mφs when compared with the inactive

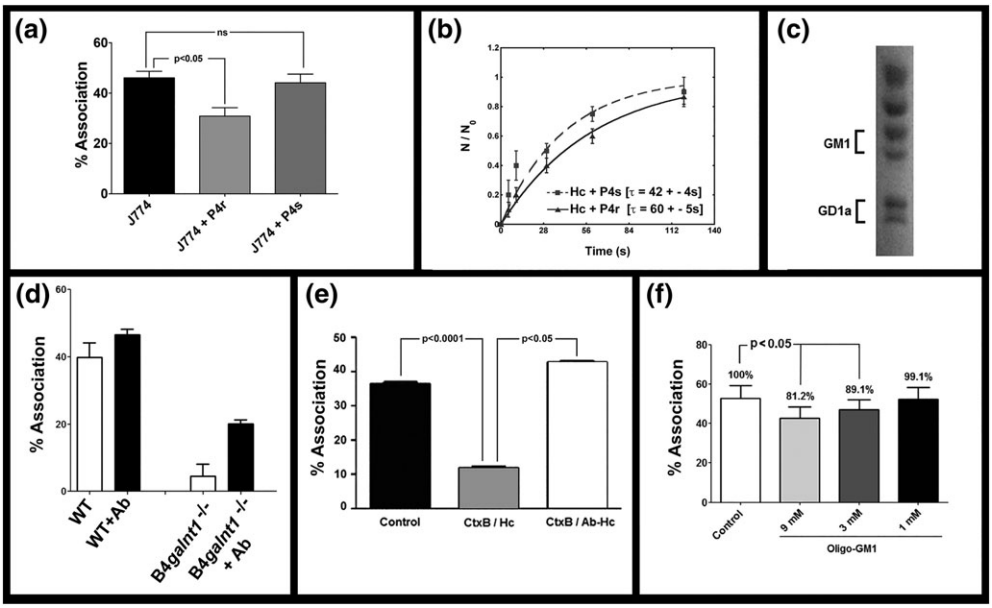

FIGURE 5 Inhibition of GSL synthesis and CtxB influences Hc-Mφ association. (a) Inhibition of GSL expression decreases fungal association to J774.16 Mφ ($P < 0.05$). Mφs treated with the CerGlcT inhibitor P4r (active isomer) for 3 days have a 70% inhibition of ganglioside expression whereas exposure to P4s (inactive isomer) had no effect (data not shown). Treated Mφs were incubated with GFP-Hc and the association index determined by FACS analysis. (b) Kinetics of Hc-Mφ adhesion measured by OT. Treatment of Mφs with P4r (Δ) results in decreased kinetics of adhesion compared with control systems (■). Characteristic time (τ) required for adhesion is shown. (c) TLC showing major gangliosides produced by J774 cells. GM1 and GD1a are indicated and were detected by immunoassays using specific mAbs (data not shown). (d) GFP-Hc yeast cells with or without opsonisation with mAb 7B6 were incubated for 45 min with WT or *B4galnt1*$^{-/-}$ peritoneal Mφs. Samples were analysed by flow cytometry. (e) Hc yeasts were incubated with J774.16 Mφs previously treated with CtxB (1 μg/ml). Binding of CtxB to Mφ cell surface inhibited fungal association (CtxB/Hc). Pretreatment of yeasts with mAbs to HSP60 reversed the effect of CtxB (CtxB/Ab-Hc). Association percentage values normalised by the control are shown (above bars). (f) Hc yeast were coincubated with oligo-GM1 and J774.16 Mφs. Inhibition of fungal association by oligo-GM1 was dose dependent. The experiments were performed at least twice with similar results

isomer (42 ± 4 s vs. 60 ± 5 s, Figure 5b). We believe treatment with P4 does not impact cytoskeleton stability because no changes were observed in F-actin (Figure S3). The ability of m-β-CD to extract macrophage gangliosides was also investigated (Figure S4). Although a small reduction was observed (approximately 21% for GM1 and approximately 25% for GD1a) when compared with P4 treatment, the results were significant, suggesting that a decrease in Hc association to macrophages could be also linked to the reduced amount of gangliosides.

2.6 | Complex gangliosides are required for Hc-Mφ association

The data indicating the participation of GSL during fungal association with Mφs led us to determine which gangliosides are synthesised by Mφs and explore their role during interaction with Hc. The resolution of polar lipids extracted from J774.16 Mφs by TLC revealed six major resorcinol-positive (sialic acid-containing) bands (Figure 5c). Based on their migration, the major gangliosides synthesised by Mφs corresponded to GM3, GM1, and GD1a, each migrating as double bands due to variations in their lipid moieties (Ando & Yu, 1984). BMDMs revealed four major resorcinol-positive bands corresponding to GM1 and GD1a (Figure S1). The presence of GM1 and GD1a was confirmed by immunostaining (data not shown). Considering that Mφ GSL levels influenced Hc interactions, we analysed the association of yeast with peritoneal Mφs (pMφs) isolated from *B4galnt1* deficient mice and wild-type (WT) mice. *B4galnt1*$^{-/-}$ mice lack the *N*-acetylgalactosaminyltransferase required for the synthesis of complex gangliosides, such as GM1 and GD1a. Instead, they accumulate truncated gangliosides, such as GM3 and GD3 (Sheikh et al., 1999). PMφs from *B4galnt1*$^{-/-}$ mice were significantly impaired in their capacity to bind Hc compared with Mφs from WT mice, showing an almost complete loss of fungal association ($P < 0.02$, Figure 5d). Hc opsonisation with anti-HSP60 mAb partially reversed the reduced capacity of *B4galnt1*$^{-/-}$ Mφs to recognise yeasts, as observed for m-β-CD treatment. These data suggest that Mφs lacking complex gangliosides have an impaired capacity to organise the cell surface apparatus required to recognise Hc. Also, only complex gangliosides, GM1 and GD1a, appear to be involved with fungal association, because GM3 accumulates in *B4galnt1*$^{-/-}$ mice.

2.7 | Cholera toxin Subunit B and oligo-GM1 inhibit Hc association with Mφs

Because the absence of complex gangliosides impaired the recognition of Hc yeasts by Mφs, we tested whether GM1 and GD1a could be additional receptors for Hc. In fact, GSL have been described as receptors for bacterial toxins, virus, and fungus (Kroken et al., 2011;

Matrosovich, Herrler, & Klenk, 2015; Oda, Terao, Sakurai, & Nagahama, 2015; Ywazaki, Maza, Suzuki, Takahashi, & Straus, 2011). In order to do that, we tested whether the Cholera toxin Subunit B (CtxB), a well-described ligand for GM1, and the lipid-free glycan derived from GM1 (oligo-GM1) would also interfere with Hc infection. Treatment with CtxB, which blocks part of the available GM1 at the J774.16 Mφ surface, significantly decreased fungal association (Figure 5e). As observed for m-β-CD treatment, opsonisation reversed the inhibition effect of CtxB. We also investigated whether the addition of GM1 could impair binding of Hc to J774.16 Mφs using soluble binding inhibition assays with different concentrations of oligo-GM1. Our results demonstrate that 1-, 3-, and 9-mM oligo-GM1 resulted in a dose-dependent reduction of association to 99%, 89%, and 81%, respectively, relative to control (Figure 5f; $P < 0.05$). Because CtxB can also modulate the architecture and dynamics of microdomains composition and function (Day & Kenworthy, 2015) and that the percentage of association inhibition using oligo-GM1 was very low, additional experiments to investigate the participation of complex gangliosides as receptors were performed. Overlay assays in ELISA and HPTLC plates using immobilised gangliosides (Lopez & Schnaar, 2006) and incubations with yeasts of Hc were developed. Under our experimental conditions, no direct association between any GSL and Hc yeasts was visualised (data not shown). These results suggest that the role of GM1 in Hc adhesion to phagocytes is accessory and probably involves the microdomains architecture and the participation of other plasma membrane components.

2.8 | Lack of complex gangliosides interferes with CD18 recruitment to lipid microdomains

Our results indicated that lipid microdomains disruption and complex gangliosides absence impaired efficient association between Hc and Mφs. However, GM1 and GD1a do not appear to be receptors for Hc yeasts. To explore possible mechanisms regulating this phenomenon, we investigated the association between complex gangliosides and CD18 recruitment to lipid microdomains using Mφs from WT and *B4galnt1*$^{-/-}$ mice. Integrin CD18 was chosen as a prototype for mechanistic evaluation because of its well-known role on Hc adhesion to Mφ (Bullock & Wright, 1987; Long et al., 2003). The CD14 receptor was also examined, because this receptor is a GPI-anchored protein expected to be enriched in lipid domains (Schmitz & Orso, 2002). The amount of CD14 in lipid microdomains fractions is similar in Mφs from both phenotypes (Figure 6a,b). Thus, this result indicated that a lack of complex gangliosides does not impair lipid microdomains assembly at the cell surface. In contrast, in comparison with Mφs from WT mice, CD18 was significantly decreased in lipid microdomains fractions isolated from *B4galnt1*$^{-/-}$. Larger amounts of CD18 were found in other fractions that do not correspond to lipid microdomains density fractions (Figure 6a,b). Remarkably, the levels of CD18 in WT and *B4galnt1*$^{-/-}$ macrophages were similar (Figure S5). Thus, these results indicated that complex gangliosides could be important for the correct maintenance of transmembrane proteins within lipid rafts, and disruption of gangliosides could interfere with Hc association.

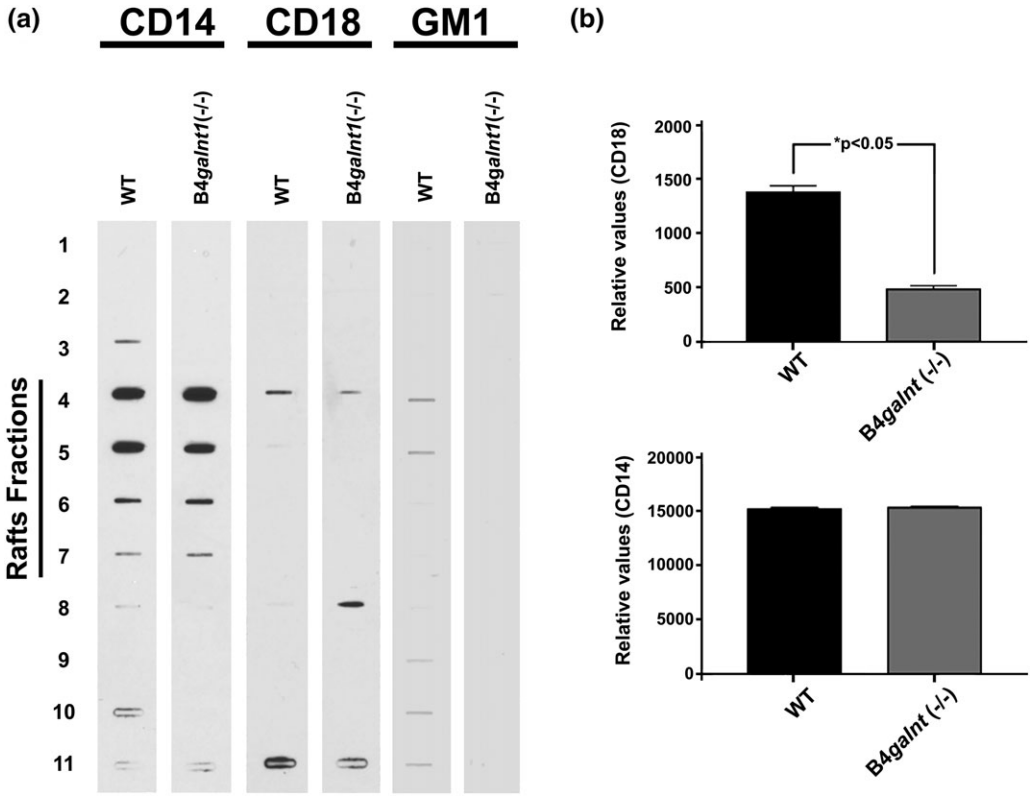

FIGURE 6 Complex gangliosides are required for correct CD18 recruitment to lipid microdomains. (a) Lipid microdomains were isolated from WT and *B4galnt1*$^{-/-}$ mice Mφs. Fractions from sucrose gradients were probed with peroxidase-conjugated antibodies to CD14 or to CD18 (Becton Dickinson). Peroxidase-labelled CtxB (Sigma) was used to detect GM1. (b) Densitometric analysis of fractions corresponding to lipids microdomains was performed using ImageJ and the relative values from one experiment are presented. Experiments were performed three times with similar results ($^{*}P < 0.05$)

2.9 | Association with Hc is reduced in CD11b$^{-/-}$ Mφs but not modified in phagocytes with reduced CD18 expression (CD18^{low})

CR3 is composed by α and β integrins (CD18 and CD11b, respectively) with well-recognised adhesive properties (Ehlers, 2000). CD18 is a major ligand for HSP60 displayed at the cell wall of Hc (Long et al., 2003). However, participation of other integrins including CD11a and CD11c cannot be ruled out (Newman, Bucher, Rhodes, & Bullock, 1990). According to Lin and colleagues, CD18 is a key protein for Hc phagocytosis by Mφs (Lin et al., 2010). The significant decrease of CD18 detection within lipid rafts isolated from Mφs lacking complex gangliosides led us to investigate the requirement of CD18 to Hc adhesion. Initially, we confirmed the reduced levels of CD18 staining in the CD18^{low} Mφ by Western Blot (Figure S6). The association index of Hc to CD18^{low} was similar to that observed for WT Mφs (Figure 7a). These results were confirmed by OT experiments, which showed that the kinetics of Hc binding to the Mφs was identical in both CD18^{low} and WT cells (data not shown). On the other hand, Mφs lacking CD11b showed a 30% decreased capacity to associate with Hc yeasts (Figure 7a). To confirm this observation, we performed additional experiments of fungus–host cell adhesion using OT, comparing Chinese hamster ovary (CHO) cells expressing the same α (CD18) and distinct β integrins (CD11a, CD11b, and CD11c, to form, respectively, the LFA1, CR3, and CR4), and observed that the rate of yeast–Mφ stable adhesion was higher for CHO expressing CD11b integrins in comparison with CHO null or expressing CD11a or CD11c integrins (Figure S7). Together, these data suggest that CD11b can also impact Hc-Mφs association.

2.10 | CD11b and CD18 colocalised with GM1 and Hc yeasts during Mφ infection

Given the potential involvement of GSL in receptor recruitment and stabilisation of Hc adhesion to Mφs, we mapped GM1, CD18, and CD11b during infection of BMDMs. We first examined the distribution of GM1 at the cell surface of Mφs. GM1 was distributed over the entire cell surface, with some punctuate staining (Figure 7b) similar to what has been published (Huang et al., 2015). We then assessed GM1, CD18, and CD11b distribution at the surface of Mφs infected with Hc. Staining with FITC-labelled CtxB was performed at 4°C to avoid Hc and CtxB internalisation and to impair reorganisation of GM1 along the Mφ cell surface (Dickens & Thompson, 1981; Kasai et al., 1976; Martin et al., 1976; Williamson, Shanahan, & Hochmuth, 1975). GM1 was again present along the entire Mφ surface, including the yeast binding sites (Figure 7b). CD11b and CD18 are distributed over the cell surface of Mφ (Huang et al., 2015). After incubation of Hc with Mφ, CD11b was found surrounding the yeast cells in a pattern similarly to that observed for GM1. Reactivity to anti-CD18 was also visualised at the interface between Hc and Mφs (Figure 7b). These results indicate that both integrins are found in lipid domains surrounding yeasts of Hc yeasts, strongly suggesting the involvement of these lipid-enriched compartments during interaction between Mφ and Hc.

3 | DISCUSSION

Lipid microdomains are nanoscale regions in the membrane that are able to compartmentalise lipids and proteins, forming platforms that coalesce and participate during membrane signalling, trafficking, and phagocytosis (Barrias, Dutra, De Souza, & Carvalho, 2007; Dykstra, Cherukuri, Sohn, Tzeng, & Pierce, 2003; Kim, Watarai, Makino, & Shirahata, 2002; Lafont & van der Goot, 2005). Exploring lipid microdomains dynamics can shed light on new mechanisms or alternatives for blocking infectious processes. Our experiments indicate that these platforms are involved with the initial kinetics of Hc-Mφ association and fungal internalisation. Using live cells, we showed that Mφs-Hc interaction induces recruitment of laterally organised lipid domains and Mφ membrane organisation, first at the site of fungus–phagocyte contact and then along the entire surface of the host cell. As the process continues, the interaction of Hc with Mφs triggers a general change in membrane organisation that apparently persists after internalisation of the fungus, potentially affecting future events of phagocyte infection. Membrane plasticity would allow recruitment of other proteins, modulating Mφs-Hc engagement and the host cell response, as suggested in a previous study (Huang et al., 2015).

We hypothesise that global membrane organisation at initial times of interaction could be associated with basal sterol levels, a

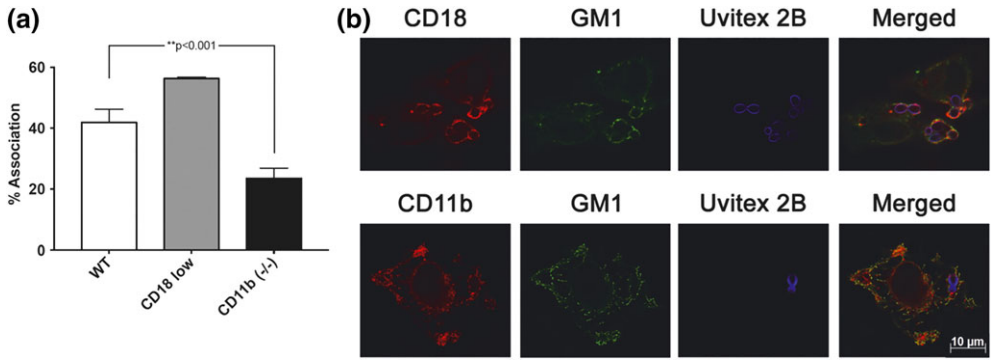

FIGURE 7 Participation of CD18 and CD11b during Hc-Mφs association. (a) GFP-Hc yeast cells were incubated for 5 min with WT, *CD18^{low}*, or *CD11b$^{-/-}$* Mφs. The association levels were analysed by flow cytometry ($^{*}P < 0.001$). (b) Bone marrow-derived murine Mφs were incubated with Uvitex 2B-labelled Hc for 15 min (moi 1:2), and the distribution of ganglioside GM1 (green), CD18 (red, upper panel), and CD11b (red, lower panel) were evaluated. The overlay images show the binding sites between Mφs and Hc by the colocalisation of integrins and GM1. Bar, 10 µm

requirement for ideal membrane plasticity (Marsh, 2009). Changes in or obstructions of microdomains components interfere with adhesion and internalisation (Riethmuller, Riehle, Grassme, & Gulbins, 2006). For example, sterol-depleted Mφs are not efficient at internalising mycobacteria (Gatfield & Pieters, 2000). In this setting, mycobacteria remained loosely attached to the sterol-depleted cell membranes, whereas control Mφs readily internalised the pathogen. In addition, a higher depletion of sterol content also impairs FcR function in Mφs during Hc adhesion suggesting that engagement and phagocytosis through FcγR are at least partially linked with lipid microdomains assembly. In fact, m-β-CD treatment of CHO cells expressing human FcγRIIA impairs binding and phagocytosis of 4.5-μm polystyrene beads covered with IgG (Vieth, Kim, Pan, Schreiber, & Worth, 2010). Although these cells are not classical phagocytes, these results confirm a possible involvement of lipid rafts during internalisation through FcγR. In our model, sterol appears to be necessary mostly during the initial events of interaction between Mφs and Hc yeasts probably through a mechanism that involves microdomain rearrangements. For longer periods of interaction, other mechanisms may compensate sterol requirement because the relative associations reach 100% even after m-β-CD treatment. In addition, disruption of the lipid microdomains was overcome in the setting of opsonised yeast, especially during the first 15 min of interaction, suggesting a more efficient association through FcR. Decreasing in association levels is usually correlated with adhesion impairment, which we also confirmed by OT analysis. However, sterol depletion also appears to influence internalisation of Hc by Mφs. Thus, normal concentrations of sterol are required for optimal adhesion and internalisation events during Mφs-Hc recognition.

Membrane cholesterol levels are a key factor in determining microdomain stability and organisation (Silvius, 2003), and GSLs constitute a second pool in membrane microdomains (Lafont & van der Goot, 2005). Although the major effect of m-β-CD is to deplete sterols from cell membranes, our results demonstrated that this treatment also reduced the presence of GSL in a minor but significant level. We then extended our studies investigating the contribution of sialic acid-containing GSL, the so-called gangliosides, during Hc-Mφs association. Inhibition of GlcCer synthesis by P4r, which affects the levels of all downstream GSLs, resulted in an effective decrease in fungal association and adhesion kinetics. Our results showed that major gangliosides synthesised by Mφs include GM3, GM1, and GD1a. Although an increase of sphingomyelin and ceramide was also observed, the changes are minimal and unlikely to influence Hc-Mφs association. To confirm the requirement for complex gangliosides during Mφs-Hc, we used Mφs from *B4galnt1*$^{-/-}$ mice, which the synthesis of complex gangliosides, including GM1 and GD1a, is impaired (Sheikh et al., 1999). Key neural functions for complex gangliosides have been suggested using these animals as models (Sheikh et al., 1999; Sun et al., 2004); however, the impact of altered ganglioside synthesis in infectious processes has not been evaluated. Because both association and adhesion kinetics were decreased when *B4galnt1*$^{-/-}$ Mφs were used, two possibilities were raised. First, depletion of GSL would disorganise complexes and modify lateral or side-by-side (*cis*-interactions) associations with other membrane molecules within lipid domains and interfere with functions of proteins such as integrins from Mφs, resulting in a lower association level with yeasts. Second, gangliosides could be coreceptors during initial steps of interaction with apposing cells (*trans*-interactions), as previously suggested for other GSL (Jimenez-Lucho, Ginsburg, & Krivan, 1990). GSLs have been reported as ligands for different pathogens, including fungi (Bergelson et al., 1982; Jimenez-Lucho et al., 1990; Krivan, Ginsburg, & Roberts, 1988; Krivan, Roberts, & Ginsburg, 1988; Superti & Donelli, 1991). In *Paracoccidioides brasiliensis*, GM1 has been shown to bind to yeast forms and to accumulate at fungal binding sites in alveolar epithelial cells (Ywazaki et al., 2011). Previous data suggested that GM1 is also recruited to sites of Hc association in host cells (Huang et al., 2015), but no function regarding the importance during the association process was determined. GM1 has also been shown to colocalised with CD44 in human brain microvascular endothelial cells interacting with *Cryptococcus neoformans* (Huang et al., 2012). In addition, Ywazaki suggested that GM3 and GM1 participate during binding and/or infection by *P. brasiliensis* (Ywazaki et al., 2011). Mobility of GM1 has been demonstrated to impact endocytosis of CtxB, a toxin that specifically binds to this GSL (Pang, Le, & Nabi, 2004). Furthermore, internalisation of *Escherichia coli* by epithelial cells requires GM1 recruitment (Kansau et al., 2004), and internalisation of the intracellular pathogen *Legionella* involves a mechanism dependent on GM1- and GPI-anchored proteins (Watarai, Makino, Fujii, Okamoto, & Shirahata, 2002).

In our model, inhibition of Hc association after exposure of host cells to CtxB might be the result of steric hindrance or lower mobility of GM1 after binding to the toxin, impairing the recruitment of these molecules to lipid microdomains along with other receptors, which consequently would stabilise the Hc-Mφ interactions. The fact that CD14 is normally enriched in lipid microdomains from *B4galnt1*$^{-/-}$ Mφs suggests that such domains are formed in the absence of complex gangliosides. Thus, Mφs-Hc interaction is dependent not only on microdomains formation but also to a well-coordinated recruitment of specific molecules, such as complex gangliosides, during their assembly. Several receptors on the Mφ surface are able to mediate interaction with Hc, including CD18, Dectin-1, and TLR (Lin et al., 2010). However, Lin et al. (2010) suggest that only CD18 is involved with Hc adhesion and internalisation in the absence of opsonins. Recently, Huang et al. (2015) demonstrated that Dectin-1 and CR3 cross-talk within lipid microdomains, which in part could explain our results. We also showed that CD18 was significantly decreased in lipid microdomains from *B4galnt1*$^{-/-}$ Mφs, which could result in loose association between the Mφ and Hc. In fact, CD18 partially colocalises with lactosylceramide (LacCer)-enriched lipid microdomains in the plasma membrane of neutrophils during phagocytosis of nonopsonised zymosan (Nakayama et al., 2008). Accordingly, CD18 is recruited to lipid microdomains, and the pretreatment of neutrophils with anti-LacCer, anti-CD11b, and lactose interferes with phagocytosis. Our results initially indicate that complex gangliosides could participate during basal CD18 recruitment to lipid microdomains in Mφs. In addition, GM1 and CD18 could cooperatively act during Hc recognition and trigger amplification of CD18 recruitment, resulting in stable adhesion and initiating signalling for fungal internalisation. In addition, OT experiments revealed that CD18^{low} Mφs support Hc adhesion as well as WT. These results indicate that low CD18 expression is sufficient for Mφs-Hc binding. Absence of CD11b culminated with

decreased but not null Hc recognition by Mφs, suggesting that intact CR3 is not essential but enhances the fungal–phagocyte association. Cell wall β-glucan could attach to the CD11b-lectin site located C-terminal to the I-domain of CD11b and induce changes in the integrin conformation with possibly increased ligand affinity (O'Brien et al., 2012; Thornton, Vetvicka, Pitman, Goldman, & Ross, 1996). Using OT, we confirmed that CHO cells expressing the heterodimers LFA-1 (CD11a/CD18) and CR4 (CD11c/CD18) were also able to support Hc binding but required a higher adhesion time (Figure S7).

Our results demonstrate that membrane microdomain composition impacts Hc recognition by Mφs. Furthermore, they are required for efficient internalisation, a step necessary to optimal Hc replication and disease development. We observed that GSL (especially GM1) and membrane microdomains are involved with integrin recruitment and potentially with stability of Hc-Mφ interactions. In addition, Hc internalisation through membrane microdomains suggests a selective retention of membrane components with potential segregation of other molecules. The lateral association between proteins and GSL could regulate Mφs function during interaction with Hc through integrin control (Jia, Howlader, & Cairo, 2016; Paller, Arnsmeier, Chen, & Woodley, 1995). Membrane microdomains and GSL composition could be then associated with the capacity of Hc to regulate internalisation, phagosome maturation, and the intracellular fate of fungus. Future studies are under development to determine whether lipid microdomains and specifically GSL could influence histoplasmosis establishment and impact the orchestration of host immune responses.

4 | EXPERIMENTAL PROCEDURES

4.1 | Fungal strains and mammalian cells culture

For phagocytic assays, we used the Mφ-like cell J774.16, derived from a reticulum cell sarcoma (ATCC TIB 67) as well as primary or derived murine cells. J774.16 cells were cultured in DMEM with 10% heat-inactivated FBS, 10% NCTC-109 medium, nonessential amino acids (1% by volume of 100× mixture, Invitrogen) and penicillin-streptomycin (1% by volume, Invitrogen). Hc G217B strain was obtained from the ATCC. Yeast cells were grown in Ham's F-12 medium at 37°C with rotatory shaking as described (Allendoerfer, Biovin, & Deepe, 1997). GFP-expressing strain G217B (GFP-Hc) was a gift from Dr. George S. Deepe (University of Cincinnati College of Medicine) and cultivated under the same conditions. Yeast were washed three times in PBS and counted by haemocytometer. For all experiments, the Mφ:yeast ratio used was 1:5. CHO cell lines stably transfected with LFA-1 (CD18/CD11a), CR1 (CD35), CR3 (CD18/CD11b), or CR4 (CD18/CD11c) were a gift from D. T. Golenbock (University of Massachusetts Medical School, Boston, Massachusetts, USA). CHO cells were cultured in Ham's F-12 medium supplemented with 1.176-g/L sodium bicarbonate and 5% heat-inactivated FBS at 37°C.

4.2 | Mice

Mice with a disrupted gene for GM2/GD2 synthase, *B4galnt1*$^{-/-}$, were generated by Dr. Richard Proia (U.S. National Institutes of Health.) and then extensively back-crossed onto a C57BL/6 background as described (Pan et al., 2005). Four- to eight-week-old female C57BL/6 CD11b$^{-/-}$ (strain B6.129S4-*Itgam*^{tm1Myd}/J) mice were purchased from Jackson Laboratory (Bar Harbor, MA). CD18^{low} (C57BL/6 genetic background) mice were donated by Prof. Lucia H. Faccioli (Universidade de São Paulo, Brazil). WT C57BL/6 mice used as control were purchased from Charles River. Animal procedures were approved by Albert Einstein College of Medicine Animal Care and Use Committees.

4.3 | BMDM and pMφs

To prepare pMφ, peritoneal cells were harvested from WT or KO mice using classic protocols (Fortier & Falk, 2001). Bone marrow cells were differentiated in vitro in the presence of RPMI with 10% FBS and 20% L929 supernatant. After 4 days the differentiation media was replaced by new one, and at the seventh day, macrophages were differentiated as confirmed by flow cytometry as F4/80^{+}/LY-6C^{-} cells.

4.4 | Laurdan confocal fluorescence microscopy and GP measurements

To investigate the formation of lipid microdomains at the sites of interaction between Hc and Mφs, Laurdan fluorescence spectroscopy combined with spatial resolution optical microscopy was used (Sanchez et al., 2007). Laurdan is a fluorescent probe that intercalates at the membrane perpendicular to the lipid bilayer and distributes equally, independent of the lipid composition of the membrane. Laurdan fluorescence spectrum shifts according to the polarity of the environment (Parasassi, De Stasio, d'Ubaldo, & Gratton, 1990; Weber & Farris, 1979). The spectral change is related to the accessibility of water in the membrane and thus to the lateral strength of the interactions between lipid chains, representing different lipid phases. This spectral change can be quantified by calculating the ratio between two different emission wavelengths. This value is called the general polarisation or GP (Parasassi et al., 1990). The GP theoretical values range from −1 to 1, but for biological membranes, it is known that GP values higher than 0.5 are characteristic of gel phase; values from 0.3 to 0.5 represent liquid organised membranes, which are characteristic of lipid microdomains; and GP values below 0.3 are presented by liquid disordered membrane domains (Parasassi et al., 1990; Sanchez et al., 2007).

BMDMs were plated in glass bottom dishes (MatTek) and incubated in medium containing 20-mM Laurdan for 10 min prior to the addition of Hc-Rho cells (see details below). Laurdan-loaded Mφs were then washed with Laurdan-free medium and imaged to establish the average GP value of the cells in the absence of Hc. Time-lapse sequences of images were acquired throughout Hc contact, interaction, and internalisation by Mφs. Time-lapse image sequences of Laurdan-labelled Mφs were acquired in a Zeiss LSM 510 META NLO microscope (Zeiss, Germany). Images were acquired simultaneously in four channels. Channels 1 and 2 were used to acquire the Laurdan-emitted fluorescence in 440 and 490 nm, respectively, Channel 3 was used to acquire transmitted light images of the Mφs as a reference, and Channel 4 was used to image the red fluorescence from Hc-labelled cells. To compare the lipid lateral organisation at the Hc–macrophage contact areas to the average

macrophage lipid organisation, we calculated the entire GP sequence from the time-lapse experiment, and the average GP values for the Mφs is calculated for each frame. To follow lipid organisation changes specifically at the site of Hc interaction, masks were obtained for each frame, representing the position of each Hc cell along the interaction process using the fluorescence images in Channel 4. The masks were applied over the GP sequence, and the average GP values for Hc contact sites were obtained for each frame. All images were acquired with a Zeiss Plan-Apochromat 63×/1.40 oil immersion objective lens. Laurdan was excited by two-photon excitation, using a MaiTai Titanium-Saphire pulsed laser (80-MHz pulse frequency, 120-fs pulse width; Spectra-Physics Newport, Mountain View, California) at 780 nm using a 680LP dichroic mirror, and fluorescence emission was measured at 440 and 490 nm, simultaneously at the META spectral detector. The emission wavelengths at the META detector were set carefully to avoid cross-talk from other fluorescence signals from the cells. Hc-Rho yeasts were used for these experiments, and fluorescence was excited at 561 nm, and emission was observed through a BP 575–615 IR band pass filter and collected in the photomultiplier tube at Channel 4. Transmitted light images of the cells were acquired during all the measurements using the 561-nm laser line simultaneously to the acquisition of the Hc-Rho image. After time-lapse sequences acquisition, GP images were calculated for each frame from the images obtained at 440 and 490 nm, as described before (Parasassi, De Stasio, Ravagnan, Rusch, & Gratton, 1991), using Equation 1 as follows:

$$GP_{corr} = \frac{(I_{440} - G \times I_{490})}{I_{440} + G \times I_{490}}. \quad (1)$$

I_{440} is the pixel intensity at 440 nm, and I_{490} corresponds to the pixel intensity at 490 nm. The G factor is used to correct possible differences in sensitivity between the two channels and is obtained from images collected in the same experimental conditions for a Laurdan solution (20 mM) in DMSO, where the GP is known to be 0.2 (Sanchez et al., 2007). Images were analysed, and GP calculations were performed in SimFCS software (Laboratory for Fluorescence Dynamics, University of California at Irvine, California, USA).

Laurdan GP images presented are from a representative experiment of three replicates. As described above, Mφs values are calculated as the average of all Laurdan signals in the image, meaning that all macrophages are being included. In our experiments, all Mφs cells in all images are in contact with at least one Hc cell. All Hc cells detected in the field are measured as a contact area, as described above. Then, considering approximately 30 Hc cells and at least 20-Mph cells detected per field, in 90 frames, we have about 2,700 measurements of Hc-Mφs contact regions per experiment, more than 60-Mph cells measured in the three replicates and about 90 contact regions followed in real time during the interaction process. It is worthy to note that the area of Mφs is much larger than the area of contact regions recovered from Hc-Rho fluorescence. As the area of the contact regions is much smaller, less pixels are used to calculate the average GP of these areas, and that is the reason of the larger variation observed for these values. Results were compared by unpaired t test and considered significantly different for $P < 0.001$. Statistics are presented in Table S2.

4.5 | Sterol enrichment at Mφs and Hc association sites

To determine whether cholesterol is recruited to fungal binding sites, J774.16 cells were used. Mφs were plated in eight-chamber polystyrene tissue-culture glass slides as described previously (Nosanchuk, Steenbergen, Shi, Deepe, & Casadevall, 2003). Hc was incubated with wheat germ agglutinin (WGA)-Alexa 546 at 1 μg/ml at RT for 1 hr, washed three times with PBS and enumerated. Yeasts were added to the wells in a Hc:Mφ ratio of 5:1 and incubated for 15 min at 37°C. After washing to remove nonadherent cells, the slides were stained with 10 μg/ml of filipin for 45 min at 4°C. WGA and filipin are probes to detect chitin oligomers and sterol, respectively. The monolayers were washed again with PBS and fixed with PF 4% for 30 min at room temperature. Slides were mounted with *n*-propylgallate, sealed under a coverslip, and then visualised by epifluorescence under an Observer Z1 microscope (Zeiss). After Z-stack acquisition, images were treated by deconvolution (Zen software—Zeiss).

4.6 | M-β-CD treatment and association index

To deplete sterol from cell surfaces, J774.16 Mφ monolayers were treated with m-β-CD. The m-β-CD stocks were prepared in serum-free DMEM. Mφs were washed once with serum-free DMEM and then incubated with different concentrations of m-β-CD (5, 10, or 20 mM) for 45 min at 37°C. After washing with serum-free medium, Mφs were used for functional assays. Different concentrations of m-β-CD were used based on previous studies showing that increasing concentrations reduce sterol content in a dose-dependent fashion (Ottico et al., 2003). After m-β-CD treatment, sterol depletion was confirmed by staining Mφs with filipin, a fluorescent sterol ligand. Cells were visualised by epifluorescence on a Zeiss Axioskop 200 inverted microscope equipped with a cooled CCD using 63× and 40× objectives. Cell viability after m-β-CD treatment was assessed as described (Abboud et al., 2009).

To measure the impact of cholesterol depletion on association, Mφs plated onto 24-well plates were cultivated with or without m-β-CD under the conditions detailed above. After m-β-CD treatment Mφs were washed with PBS three times and then incubated with GFP-Hc for 15 or 45 min at 37°C (multiplicity of infection 5 Hc: 1 Mφ). Plates were washed, and infected Mφs displaying fluorescent yeast were measured using a FACSCalibur flow cytometer (BD Biosciences). Expression of CD18 was compared between control and m-β-CD-treated cells also using flow cytometry. For these experiments, Mφs (1×10^6 cells) were detached from flasks using 0.053-mM EDTA at room temperature for 5 min and then washed again with PBS. Cells were fixed with PF 4% for 30 min at room temperature. After blocking non-specific sites using 1% BSA, anti-mouse PE-conjugated CD18 (1 μg/ml; Biolegend, clone M18/2) or anti-mouse APC-conjugated CD11b (1 μg/ml; eBioscience, clone M1/70) was added, and the cells incubated for 1 hr at room temperature. Negative isotype controls (IgG1 and IgG2a antibodies conjugated to APC, BIO-RAD) were used as controls. A total of 10,000 events were recorded for each flow cytometer analysis. The percentage of Hc-associated Mφs and the

association index (total number of Mφs containing Hc adhered and/or internalised) was obtained for each experimental condition (Cordero et al., 2016). All experiments were performed three times with consistent results. A control experiment without m-β-CD treatment was performed, and the infection rate normalised as 100%.

4.7 | OTs experiments

We used OTs to access the interaction between Hc and Mφs. All the experimental procedures used were adapted from Guimaraes et al. (2011). Briefly, a yeast cell suspension was trapped with the OTs and allowed to interact with an adhered Mφ for periods of time ranging from 5 to 300 s. Then the microscope stage was set to move with a controlled velocity in order to detach the optically trapped yeast cell from the Mφ surface. The maximum optical force in these experiments was set to be in the order of 20 pN (Viana et al., 2007). If the Hc–host cell interactions were stronger than the maximum force, the cells remain in contact and we considered this event as a positive adhesion event. The relative adhesion was defined as the number of positive adhesion events (N) divided by the total number of attempts (N_0). The relative adhesion was determined for each time point and each experimental condition used. The characteristic time (τ) was defined as the time required for 63% of the interactions to be positive in all the attempts tested, and it was determined based on the best fit for all the curves obtained according to the equation:

$$\frac{N}{N_0} = 1 - \exp\left(-\frac{t}{\tau}\right). \quad (2)$$

The error bars in the relative adhesion were determined as half the difference between the maximum and minimum values for each time interval in 30 events performed with three different samples. The error bars in the characteristic time were obtained using the best curve fit for Equation (2) and also weighting the data with the errors for the relative adhesion. All curve fits were obtained using the Kaleidagraph software (Synergy Software). To investigate the sterol requirement, four experimental conditions were used: (a) Hc with control Mφs, (b) Hc with 10-mM m-β-CD-treated Mφs, (c) opsonised Hc with control Mφs, and (d) opsonised Hc with 10-mM m-β-CD-treated Mφs. To determine the influence of GSL, Mφs were treated with P4 as described below. Requirement of CD18 was studied using Mφs expressing very low amounts of this integrin (Sorgi et al., 2009), and for the coreceptors of distinct integrins, we have used CHO cells transfected with LFA-1 (CD18/CD11a), CR1 (CD35), CR3 (CD18/CD11b), or CR4 (CD18/CD11c).

4.8 | Influence of m-β-CD and CtxB on phagocytosis of Hc by Mφs

We tested whether m-β-CD influenced internalisation of Hc by Mφs according to our previously published protocol, with minor adaptations (Shi et al., 2008). Briefly, Mφs were plated at 2×10^5 cells/well in an eight-chamber polystyrene tissue-culture glass slide (Becton Dickinson) and grown overnight. Hc were preincubated with 8-μg/ml NHS-Rho (molecular probes) at 4°C for 1 hr. After several washes with PBS to remove excess NHS-Rho, fungal cells were plated onto Mφ monolayers, with or without m-β-CD treatment, as described previously. Cells were then moved back to 37°C and incubated with NHS-Rho-labelled Hc (Hc-Rho). After incubation, nonattached Hc were removed by washing the preparation with PBS. The monolayers were then incubated with Uvitex B (100 μg/ml in PBS), a fluorescent dye that binds specifically to chitin on the Hc cell wall. Cells were washed again with PBS and then fixed with PF 4% for 30 min at room temperature. To evaluate the effect of fungal opsonisation during this interaction, Hc were incubated with MAb to HSP60 (50 μg/ml of mAb) and then added to the Mφ monolayer. After fixing with PF 4%, the slides were washed with PBS, sealed under a coverslip and visualised by epifluorescence. All yeast cells fluoresced red, and only noninternalised Hc also fluoresced blue, because Uvitex B is excluded from live Mφs (Levitz, DiBenedetto, & Diamond, 1987). In each system, at least 300 Mφs were counted, and the percentage of association number was determined. From infected Mφs, we determined the percentage of adherent and internalised Hc.

4.9 | P4 treatment of Mφs

To estimate the participation of GSL expressed at Mφ surface during interaction with Hc, we inhibited GlcCer formation, the first step during gangliosides biosynthesis (Fox et al., 2001). Mφs were incubated for 3 days with 1-μM P4r, a small molecular weight inhibitor of the enzyme ceramide:glucosyltransferase (Cer:GlcT). After treatment, Mφs were washed with serum-free medium and used to interact with GFP-Hc as described. The association index (total number of Mφs containing Hc adhered and/or internalised) was obtained for each experimental condition as described above. Control experiments used an inactive isomer, P4s. OT experiments were developed as mentioned above. The expression of gangliosides after P4r treatment was determined (see below) and compared with control. P4r and P4s were synthesised by Dr. D. Meyers, Synthetic Core Facility, The Johns Hopkins School of Medicine. To evaluate the effect of P4 on the cytoskeleton, Mφs were plated at 5×10^5 cells/well in an eight-chamber polystyrene tissue-culture glass slide (Becton Dickinson) and treated with P4r or P4s as described above. After 3 days of treatment, cells were washed with PBS and then incubated with phalloidin-FITC (Sigma-Aldrich) and DAPI (1 μg/ml; Sigma-Aldrich) for 1 hr. Mφs were washed with PBS; slides were mounted with *n*-propylgallate, sealed under a coverslip, and then visualised by epifluorescence under an Observer Z1 microscope (Zeiss). Experiments were performed twice with consistent results.

4.10 | Lipid extraction

Total lipids were extracted according to Schnaar (Schnaar & Needham, 1994). Mφs with or without P4r (1-phenyl-2-palmitoylamino-3-pyrrolidino-1-propanol) or m-β-CD were washed with cold PBS and removed from the Petri dishes with a scrapper. The cells were collected by centrifugation at 4°C and suspended in 3 ml of ice-cold water (W). Eight millilitres of methanol (M) was added and the suspension vigorously mixed. Chloroform (C; 4 ml) was added to the system

reaching a final proportion of C-M-W (4:8:3). After 2 hr under agitation at room temperature, the suspension was centrifuged, and the pellet extracted again with the same solvent mixture (C-M-W; 4:8:3). The pellet was dried at room temperature and then solubilised with 3–5 ml of NaOH 0.1 M, and the total protein content was determined using Pierce BCA Protein Assay Kit (Thermo Fischer Scientific, USA). Protein content was used to normalise the samples. The lipidic extracts were combined, and water was added to the supernatant to reach a final concentration of C-M-W (4:8:5.6). The suspension was mixed, and a biphasic system formed. The upper phase containing the polar lipids, including the gangliosides, was submitted to reverse phase chromatography (tC18 SepPak Plus cartridges) to remove salts and other polar contaminants. Cartridges were previously washed with 3 ml of water, M-W (1:1), methanol, and M-W (1:1) again. The upper phase was loaded, and the cartridges were washed with 3 ml of M-W (1:2) and M-W (1:1). GSLs were eluted with 3 ml of methanol. The methanol eluant (from the upper phase) and the whole lower phase, enriched in ceramide and sphingomyelin, were dried under N_2 and resolved by thin layer chromatography (TLC) as described below.

4.11 | Thin layer chromatography

The fraction eluted in methanol was solubilised in C-M-W (4:8:3), and the lower phase was solubilised in chloroform. Samples were then spotted onto TLC plates. TLC was performed on silica gel plates in proper solvent systems according to each class of lipids to be investigated. Ceramide analysis was developed in a solvent system consisting of C-M-W (80:10:1; van Echten-Deckert, 2000). Cupric sulfate in aqueous phosphoric acid was sprayed over the TLC plate for further band visualisation after heating at 180°C for 15 min. Lipid bands, including ceramide, appear brown against a white background (van Echten-Deckert, 2000). Ceramide from bovine brain was used as a standard. To identify sphingomyelin, the lipids from lower phase were resolved using C-M-W (65:25:4). TLCs were exposed to iodine in chambers saturated with iodine crystals. Bands appear yellow against a white background. Sphingomyelin from bovine brain was used as a standard. Gangliosides were resolved in solvent system containing C-M-0.25% aqueous KCl (60:35:8; Schnaar & Needham, 1994). Plates were sprayed with resorcinol/HCl reagent and heated at 125°C for 20 min (Schnaar & Needham, 1994). Gangliosides were visualised as purple spots. A mixture containing bovine brain gangliosides was used as a standard.

4.12 | Immunostaining of gangliosides

To confirm the presence of GM1 and GD1a (respectively mono and disialo species of gangliosides) on lipid extracts of J774.16 Mφs, we performed an immunostaining assay using monoclonal antibodies to GM1 and GD1a (Schnaar et al., 2002). GSLs were resolved by TLC as above, and the plate was dipped in a solution of 0.2% polyisobutyl methacrylate (Aldrich) in hexane for 30 s. The plate was dried, sprayed with PBS, and blocked for nonspecific binding with 10-mg/ml BSA in PBS for 1 hr at room temperature. After washing with PBS three times, the plate was incubated with antibodies to the gangliosides (2 μg/ml) for 2 hr at room temperature followed by incubation with a secondary alkaline phosphatase-conjugated anti-mouse IgG (1 μg/ml) under the same conditions. The plate was washed three times with PBS and then developed by using Sigma Fast NBT-BCIP according to the manufacturer's instructions. Reactive bands (purple) were compared with standards resolved at the same time and conditions but developed with resorcinol/HCl reagent.

4.13 | Influence of P4, complex gangliosides, CD11b, CD18, CtxB, and oligo-GM1 during Mφs and Hc association

GM1-oligosaccharides (oligo-GM1) were generated by treatment of GM1 with a specific ceramide glycanase (Calbiochem; Zhou, Li, Laine, Huang, & Li, 1989). To investigate whether P4 treatment, absence of complex gangliosides, and CD11b and CD18 are required for Mφs to associate with Hc, we used primary Mφs treated with P4 and Mφs derived from *B4galnt1*$^{-/-}$, CD11b$^{-/-}$, or CD18^{low} mice. CtxB is a standard ligand for GM1 and has been extensively used as a lipid raft marker (Vyas, Patel, Vyas, & Schnaar, 2001). To access the effect of CTxB, we treated Mφs with 1 μg/ml of CTxB for 45 min at 4°C before incubation with Hc. According to the manufacturer, this concentration achieves 50% saturation of GM1-coated plates. Mφs were washed with PBS three times and then incubated with GFP-Hc for 45 min at 37°C (multiplicity of infection 5 Hc: 1 Mφ). In another set of experiments, oligo-GM1 and GFP-Hc were coincubated with Mφs for 1 hr. Association indexes were determined by flow cytometry as described above (Cordero et al., 2016). In addition, some systems where fungal cells were opsonised with anti-HSP60 (13B7 or 7B6; Guimaraes, Frases, Gomez, Zancope-Oliveira, & Nosanchuk, 2009) or M antigen-specific mAbs (Guimaraes, Hamilton, de, Nosanchuk, & Zancope-Oliveira, 2008) were also tested to evaluate whether opsonisation would impact infection. The percentage of associated Mφs was obtained for each experimental condition. All experiments were performed three times with consistent results.

4.14 | Lipid microdomains isolation and dot-blot experiments

To analyse the content of CD18 and CD14 in lipid microdomains, we used BMDMs from WT and *B4galnt1*$^{-/-}$ mice. The protocol published by Takeushi and colleagues was used to prepare the Mφs (Takeuchi et al., 1999). Briefly, femur and tibia were removed; the tissue was removed by scalping and briefly washed in 70% ethanol. After cutting both sides, the bone marrow was flushed with PBS and cells gently homogenised. Precursors cells were seeded at 2×10^6 per 100-mm dish in 10-ml complete medium (DMEM, supplemented with 10% FCS, l-glutamine, HEPES, β_2-mercaptoethanol, and penicillin/streptomycin) with 20% conditioned medium (containing M-CSF) harvested from L929 fibroblast cultured cells. After 7 days, Mφs were harvested and used to prepare lipid microdomains according to DeBruin et al. (2005) with minor modifications. Cells were washed in TNE buffer (25-mM Tris/HCl [pH 7.4], 150-mM NaCl) and the pellets lysed in 250 μl of the same buffer containing 1% triton-

X-100 and a protease inhibitor cocktail (Sigma) for 30 min at 4°C. Lysates were mixed with equal volume of 80% sucrose (*w*/*v*) in TNE buffer and then transferred to a SW41 centrifuge tube. The samples was homogenised an then overlaid sequentially with 40% (3.5 ml), 35% (5 ml), and 5% (3.5 ml) of sucrose in TNE and centrifuged at 100,000 *g* for 18 hr at 4°C. Eleven fractions of 1 ml each were sequentially collected from the top and analysed for the presence of GM1 (lipid raft marker), CD14, and CD18. Aliquots of each fraction were spotted on nitrocellulose membrane (Millipore, Bedford, MA) by using a dot-blot equipment (Pharmacia, USA). Fraction 12, overloaded with nonrafts proteins, was not spotted. After blocking, the membrane was overlaid with peroxidase-linked CtxB or monoclonal antibodies to CD14 and CD18 (BD Biosciences), followed by a secondary conjugated to peroxidase. Membranes were washed and developed by enhanced chemiluminescence (Pierce, Rockford, IL) or DAB peroxidase solution. The spots were quantified using the ImageJ software (NIH).

4.15 | Surface distribution of GM1, CD18, and CD11b during interaction of Hc and Mφs

To determine whether GM1 was recruited to fungal binding sites at the BMDM surface, labelling with FITC-conjugated CtxB was used. Mφs were plated in eight-chamber polystyrene tissue-culture glass slides as described previously (Nosanchuk et al., 2003). Hc previously incubated with Uvitex 2B (Chaka et al., 1995) were added to the wells in a Hc:Mφ ratio of 5:1 and incubated for 15 or 45 min at 37°C. After washing to remove nonadherent cells, the slides were incubated with FITC-conjugated CtxB (1 μg/ml in PBS-BSA 1%) for 45 min at 4°C. The monolayers were washed again with PBS and fixed with PF 4% for 30 min at room temperature. After blocking non-specific sites using 1% BSA, anti-mouse CD18 (1 μg/ml; BD Bioscience**)** or and anti-mouse CD11b (1 μg/ml; BD Bioscience) were separately incubated in different slides for 1 hr at room temperature. After extensive washing, a goat anti-IgG Alexa 546 (Invitrogen) was incubated for 1 hr. Slides were mounted with *n*-propylgallacte, sealed under a coverslip, and then visualised by epifluorescence under an Observer Z1 microscope (Zeiss). After Z-stack acquisition, images were treated by deconvolution (Zen software—Zeiss).

4.16 | CD18 levels in macrophages from WT and B4galnt1$^{-/-}$ mice

Mφs from WT and *B4galnt1*$^{-/-}$ mice (1 × 10^6 cells) were incubated with PE-conjugated anti-mouse CD18 as described above, and 10,000 events were recorded for flow cytometer analysis. All experiments were performed three times with consistent results.

4.17 | Statistical analysis

All statistical analyses were performed using GraphPad Prism 6, version 5.02, for Windows (GraphPad Software).

ACKNOWLEDGEMENTS

A. J. G. and L. N. were supported in part by an Interhemispheric Research Training Grant in Infectious Diseases, Fogarty International Center (NIH D43-TW007129). A. J. G. and J. D. N. were supported in part by NIH AI056070-01A2 and the Center for AIDS Research at the Albert Einstein College of Medicine and Montefiore Medical Center (NIH AI-51519). A. J. G., L. N., M. L. R., B. P., N. B. V., and D. Z-M. are supported by grants from Conselho Nacional de Desenvolvimento Tecnológico (CNPq, Brazil) and Fundação Carlos Chagas Filho de Amparo à Pesquisa do Estado do Rio de Janeiro (FAPERJ, Brazil). L. N. was also supported by CAPES-Fulbright (Visiting Scientist/Visiting Professor Scholar Program). Mutant mice and ganglioside oligosaccharides were generated with support from the National Institutes of Health (NS037096). The authors thank Dr. Steven U. Walkley (Department of Neuroscience, AECOM) and Lucia Faccioli (USP, Riberião Preto) for kindly providing us with *B4galnt1*$^{-/-}$ and CD18^{low} mice, respectively.

CONFLICTS OF INTEREST

The authors state that there are no conflicts of interests.

ORCID

Allan J. Guimarães https://orcid.org/0000-0002-2856-9667
Luis R. Martinez https://orcid.org/0000-0001-6372-6501
Leonardo Nimrichter https://orcid.org/0000-0001-9281-6856

REFERENCES

Abboud, N., De Jesus, M., Nakouzi, A., Cordero, R. J., Pujato, M., Fiser, A., et al. (2009). Identification of linear epitopes in Bacillus anthracis protective antigen bound by neutralizing antibodies. *The Journal of Biological Chemistry*, *284*, 25077–25086. https://doi.org/10.1074/jbc.M109.022061

Allendoerfer, R., Biovin, G. P., & Deepe, G. S. Jr. (1997). Modulation of immune responses in murine pulmonary histoplasmosis. *The Journal of Infectious Diseases*, *175*, 905–914. https://doi.org/10.1086/513989

Ando, S., & Yu, R. K. (1984). Fatty acid and long-chain base composition of gangliosides isolated from adult human brain. *Journal of Neuroscience Research*, *12*, 205–211. https://doi.org/10.1002/jnr.490120208

Barrias, E. S., Dutra, J. M., De Souza, W., & Carvalho, T. M. (2007). Participation of macrophage membrane rafts in Trypanosoma cruzi invasion process. *Biochemical and Biophysical Research Communications*, *363*, 828–834. https://doi.org/10.1016/j.bbrc.2007.09.068

Bergelson, L. D., Bukrinskaya, A. G., Prokazova, N. V., Shaposhnikova, G. I., Kocharov, S. L., Shevchenko, V. P., … Fomina-Ageeva, E. V. (1982). Role of gangliosides in reception of influenza virus. *European Journal of Biochemistry*, *128*, 467–474.

Brown, D. A., & London, E. (2000). Structure and function of sphingolipid- and cholesterol-rich membrane rafts. *The Journal of Biological Chemistry*, *275*, 17221–17224. https://doi.org/10.1074/jbc.R000005200

Bullock, W. E., & Wright, S. D. (1987). Role of the adherence-promoting receptors, CR3, LFA-1, and p150,95, in binding of Histoplasma capsulatum by human macrophages. *The Journal of Experimental Medicine*, *165*, 195–210. https://doi.org/10.1084/jem.165.1.195

Cano, M. V., & Hajjeh, R. A. (2001). The epidemiology of histoplasmosis: A review. *Seminars in Respiratory Infections*, *16*, 109–118. https://doi.org/10.1053/srin.2001.24241

Chaka, W., Scharringa, J., Verheul, A. F., Verhoef, J., Van Strijp, A. G., & Hoepelman, I. M. (1995). Quantitative analysis of phagocytosis and killing of Cryptococcus neoformans by human peripheral blood

mononuclear cells by flow cytometry. *Clinical and Diagnostic Laboratory Immunology*, *2*, 753–759.

Cordero, R. J., Liedke, S. C., de, S. A. G. R., Martinez, L. R., Nimrichter, L., Frases, S., et al. (2016). Enhanced virulence of Histoplasma capsulatum through transfer and surface incorporation of glycans from Cryptococcus neoformans during co-infection. *Scientific Reports*, *6*, 21765. https://doi.org/10.1038/srep21765

Cuschieri, J., Billigren, J., & Maier, R. V. (2006). Endotoxin tolerance attenuates LPS-induced TLR4 mobilization to lipid rafts: A condition reversed by PKC activation. *Journal of Leukocyte Biology*, *80*, 1289–1297. https://doi.org/10.1189/jlb.0106053

Das, T., Sa, G., Hilston, C., Kudo, D., Rayman, P., Biswas, K., … Tannenbaum, C. (2008). GM1 and tumor necrosis factor-alpha, overexpressed in renal cell carcinoma, synergize to induce T-cell apoptosis. *Cancer Research*, *68*, 2014–2023. https://doi.org/10.1158/0008-5472.CAN-07-6037

Day, C. A., & Kenworthy, A. K. (2015). Functions of cholera toxin B-subunit as a raft cross-linker. *Essays in Biochemistry*, *57*, 135–145. https://doi.org/10.1042/bse0570135

DeBruin, L. S., Haines, J. D., Wellhauser, L. A., Radeva, G., Schonmann, V., Bienzle, D., & Harauz, G. (2005). Developmental partitioning of myelin basic protein into membrane microdomains. *Journal of Neuroscience Research*, *80*, 211–225. https://doi.org/10.1002/jnr.20452

Dickens, B. F., & Thompson, G. A. Jr. (1981). Rapid membrane response during low-temperature acclimation. Correlation of early changes in the physical properties and lipid composition of Tetrahymena microsomal membranes. *Biochimica et Biophysica Acta*, *644*, 211–218. https://doi.org/10.1016/0005-2736(81)90377-1

Dykstra, M., Cherukuri, A., Sohn, H. W., Tzeng, S. J., & Pierce, S. K. (2003). Location is everything: Lipid rafts and immune cell signaling. *Annual Review of Immunology*, *21*, 457–481. https://doi.org/10.1146/annurev.immunol.21.120601.141021

Ehlers, M. R. (2000). CR3: A general purpose adhesion-recognition receptor essential for innate immunity. *Microbes and Infection/Institut Pasteur*, *2*, 289–294. https://doi.org/10.1016/S1286-4579(00)00299-9

Fortier, A. H., & Falk, L. A. (2001). Isolation of murine macrophages. *Curr Protoc Immunol Chapter 14*, *Unitas*, *14*, 11.

Fox, D. A., He, X., Abe, A., Hollander, T., Li, L. L., Kan, L., … Kozarsky, K. (2001). The T lymphocyte structure CD60 contains a sialylated carbohydrate epitope that is expressed on both gangliosides and glycoproteins. *Immunological Investigations*, *30*, 67–85. https://doi.org/10.1081/IMM-100104017

Gatfield, J., & Pieters, J. (2000). Essential role for cholesterol in entry of mycobacteria into macrophages. *Science*, *288*, 1647–1650. https://doi.org/10.1126/science.288.5471.1647

Gaus, K., Gratton, E., Kable, E. P., Jones, A. S., Gelissen, I., Kritharides, L., & Jessup, W. (2003). Visualizing lipid structure and raft domains in living cells with two-photon microscopy. *Proceedings of the National Academy of Sciences of the United States of America*, *100*, 15554–15559. https://doi.org/10.1073/pnas.2534386100

Goluszko, P., Popov, V., Wen, J., Jones, A., & Yallampalli, C. (2008). Group B streptococcus exploits lipid rafts and phosphoinositide 3-kinase/Akt signaling pathway to invade human endometrial cells. *American Journal of Obstetrics and Gynecology*, *199*(548), e541–e549.

Grassme, H., Jendrossek, V., Riehle, A., von Kurthy, G., Berger, J., Schwarz, H., et al. (2003). Host defense against Pseudomonas aeruginosa requires ceramide-rich membrane rafts. *Nature Medicine*, *9*, 322–330. https://doi.org/10.1038/nm823

Guimaraes, A. J., Frases, S., Gomez, F. J., Zancope-Oliveira, R. M., & Nosanchuk, J. D. (2009). Monoclonal antibodies to heat shock protein 60 alter the pathogenesis of Histoplasma capsulatum. *Infection and Immunity*, *77*, 1357–1367. https://doi.org/10.1128/IAI.01443-08

Guimaraes, A. J., Frases, S., Pontes, B., de Cerqueira, M. D., Rodrigues, M. L., Viana, N. B., et al. (2011). Agglutination of Histoplasma capsulatum by IgG monoclonal antibodies against Hsp60 impacts macrophage effector functions. *Infection and Immunity*, *79*, 918–927. https://doi.org/10.1128/IAI.00673-10

Guimaraes, A. J., Hamilton, A. J., de, M. G. H. L., Nosanchuk, J. D., & Zancope-Oliveira, R. M. (2008). Biological function and molecular mapping of M antigen in yeast phase of Histoplasma capsulatum. *PLoS One*, *3*, e3449. https://doi.org/10.1371/journal.pone.0003449

Hakomori, S. (2003). Structure, organization, and function of glycosphingolipids in membrane. *Current Opinion in Hematology*, *10*, 16–24. https://doi.org/10.1097/00062752-200301000-00004

Huang, J. H., Lin, C. Y., Wu, S. Y., Chen, W. Y., Chu, C. L., Brown, G. D., … Wu-Hsieh, B. A. (2015). CR3 and dectin-1 collaborate in macrophage cytokine response through association on lipid rafts and activation of Syk-JNK-AP-1 pathway. *PLoS Pathogens*, *11*, e1004985. https://doi.org/10.1371/journal.ppat.1004985

Huang, S. H., Wu, C. H., Chang, Y. C., Kwon-Chung, K. J., Brown, R. J., & Jong, A. (2012). Cryptococcus neoformans-derived microvesicles enhance the pathogenesis of fungal brain infection. *PLoS One*, *7*, e48570. https://doi.org/10.1371/journal.pone.0048570

Ilangumaran, S., & Hoessli, D. C. (1998). Effects of cholesterol depletion by cyclodextrin on the sphingolipid microdomains of the plasma membrane. *The Biochemical Journal*, *335*(Pt 2), 433–440. https://doi.org/10.1042/bj3350433

Jia, F., Howlader, M. A., & Cairo, C. W. (2016). Integrin-mediated cell migration is blocked by inhibitors of human neuraminidase. *Biochimica et Biophysica Acta*, *1861*, 1170–1179. https://doi.org/10.1016/j.bbalip.2016.06.013

Jimenez-Lucho, V., Ginsburg, V., & Krivan, H. C. (1990). Cryptococcus neoformans, Candida albicans, and other fungi bind specifically to the glycosphingolipid lactosylceramide (Gal beta 1-4Glc beta 1-1Cer), a possible adhesion receptor for yeasts. *Infection and Immunity*, *58*, 2085–2090.

Kainu, V., Hermansson, M., & Somerharju, P. (2010). Introduction of phospholipids to cultured cells with cyclodextrin. *Journal of Lipid Research*, *51*, 3533–3541. https://doi.org/10.1194/jlr.D009373

Kalischuk, L. D., Inglis, G. D., & Buret, A. G. (2009). Campylobacter jejuni induces transcellular translocation of commensal bacteria via lipid rafts. *Gut Pathog*, *1*, 2. https://doi.org/10.1186/1757-4749-1-2

Kansau, I., Berger, C., Hospital, M., Amsellem, R., Nicolas, V., Servin, A. L., & Bernet-Camard, M. F. (2004). Zipper-like internalization of Dr-positive Escherichia coli by epithelial cells is preceded by an adhesin-induced mobilization of raft-associated molecules in the initial step of adhesion. *Infection and Immunity*, *72*, 3733–3742. https://doi.org/10.1128/IAI.72.7.3733-3742.2004

Kasai, R., Kitajima, Y., Martin, C. E., Nozawa, Y., Skriver, L., & Thompson, G. A. Jr. (1976). Molecular control of membrane properties during temperature acclimation. Membrane fluidity regulation of fatty acid desaturase action? *Biochemistry*, *15*, 5228–5233. https://doi.org/10.1021/bi00669a005

Kauffman, C.A. (2009). Histoplasmosis. *Clinics in Chest Medicine 30*, 217–225, v, https://doi.org/10.1016/j.ccm.2009.02.002

Kim, S., Watarai, M., Makino, S., & Shirahata, T. (2002). Membrane sorting during swimming internalization of Brucella is required for phagosome trafficking decisions. *Microbial Pathogenesis*, *33*, 225–237. https://doi.org/10.1006/mpat.2002.0531

Krivan, H. C., Ginsburg, V., & Roberts, D. D. (1988). Pseudomonas aeruginosa and Pseudomonas cepacia isolated from cystic fibrosis patients bind specifically to gangliotetraosylceramide (asialo GM1) and gangliotriaosylceramide (asialo GM2). *Archives of Biochemistry and Biophysics*, *260*, 493–496. https://doi.org/10.1016/0003-9861(88)90473-0

Krivan, H. C., Roberts, D. D., & Ginsburg, V. (1988). Many pulmonary pathogenic bacteria bind specifically to the carbohydrate sequence GalNAc beta 1-4Gal found in some glycolipids. *Proceedings of the National Academy of Sciences of the United States of America*, *85*, 6157–6161. https://doi.org/10.1073/pnas.85.16.6157

Kroken, A. R., Karalewitz, A. P., Fu, Z., Baldwin, M. R., Kim, J. J., & Barbieri, J. T. (2011). Unique ganglioside binding by botulinum neurotoxins C and D-SA. *The FEBS Journal*, *278*, 4486–4496. https://doi.org/10.1111/j.1742-4658.2011.08166.x

Lafont, F., & van der Goot, F. G. (2005). Bacterial invasion via lipid rafts. *Cellular Microbiology*, *7*, 613–620. https://doi.org/10.1111/j.1462-5822.2005.00515.x

Levitz, S. M., DiBenedetto, D. J., & Diamond, R. D. (1987). A rapid fluorescent assay to distinguish attached from phagocytized yeast particles. *Journal of Immunological Methods*, *101*, 37–42. https://doi.org/10.1016/0022-1759(87)90213-4

Lin, J. S., Huang, J. H., Hung, L. Y., Wu, S. Y., & Wu-Hsieh, B. A. (2010). Distinct roles of complement receptor 3, Dectin-1, and sialic acids in murine macrophage interaction with Histoplasma yeast. *Journal of Leukocyte Biology*, *88*, 95–106. https://doi.org/10.1189/jlb.1109717

Long, K. H., Gomez, F. J., Morris, R. E., & Newman, S. L. (2003). Identification of heat shock protein 60 as the ligand on Histoplasma capsulatum that mediates binding to CD18 receptors on human macrophages. *Journal of Immunology*, *170*, 487–494. https://doi.org/10.4049/jimmunol.170.1.487

Lopez, P. H., & Schnaar, R. L. (2006). Determination of glycolipid-protein interaction specificity. *Methods in Enzymology*, *417*, 205–220. https://doi.org/10.1016/S0076-6879(06)17015-9

Marsh, D. (2009). Cholesterol-induced fluid membrane domains: A compendium of lipid-raft ternary phase diagrams. *Biochimica et Biophysica Acta*, *1788*, 2114–2123. https://doi.org/10.1016/j.bbamem.2009.08.004

Martin, C. E., Hiramitsu, K., Kitajima, Y., Nozawa, Y., Skriver, L., & Thompson, G. A. (1976). Molecular control of membrane properties during temperature acclimation. Fatty acid desaturase regulation of membrane fluidity in acclimating Tetrahymena cells. *Biochemistry*, *15*, 5218–5227. https://doi.org/10.1021/bi00669a004

Matrosovich, M., Herrler, G., & Klenk, H. D. (2015). Sialic acid receptors of viruses. *Topics in Current Chemistry*, *367*, 1–28. https://doi.org/10.1007/128_2013_466

Maza, P. K., Straus, A. H., Toledo, M. S., Takahashi, H. K., & Suzuki, E. (2008). Interaction of epithelial cell membrane rafts with Paracoccidioides brasiliensis leads to fungal adhesion and Src-family kinase activation. *Microbes and Infection*, *10*, 540–547. https://doi.org/10.1016/j.micinf.2008.02.004

Murphy, S. C., Hiller, N. L., Harrison, T., Lomasney, J. W., Mohandas, N., & Haldar, K. (2006). Lipid rafts and malaria parasite infection of erythrocytes. *Molecular Membrane Biology*, *23*, 81–88. https://doi.org/10.1080/09687860500473440

Nakayama, H., Yoshizaki, F., Prinetti, A., Sonnino, S., Mauri, L., Takamori, K., … Iwabuchi, K. (2008). Lyn-coupled LacCer-enriched lipid rafts are required for CD11b/CD18-mediated neutrophil phagocytosis of nonopsonized microorganisms. *Journal of Leukocyte Biology*, *83*, 728–741. https://doi.org/10.1189/jlb.0707478

Newman, S. L. (1999). Macrophages in host defense against Histoplasma capsulatum. *Trends in Microbiology*, *7*, 67–71. https://doi.org/10.1016/S0966-842X(98)01431-0

Newman, S. L., Bucher, C., Rhodes, J., & Bullock, W. E. (1990). Phagocytosis of Histoplasma capsulatum yeasts and microconidia by human cultured macrophages and alveolar macrophages. Cellular cytoskeleton requirement for attachment and ingestion. *The Journal of Clinical Investigation*, *85*, 223–230. https://doi.org/10.1172/JCI114416

Nicholson, K. M., Quinn, D. M., Kellett, G. L., & Warr, J. R. (1999). Preferential killing of multidrug-resistant KB cells by inhibitors of glucosylceramide synthase. *British Journal of Cancer*, *81*, 423–430. https://doi.org/10.1038/sj.bjc.6690711

Nosanchuk, J. D., Steenbergen, J. N., Shi, L., Deepe, G. S. Jr., & Casadevall, A. (2003). Antibodies to a cell surface histone-like protein protect against Histoplasma capsulatum. *The Journal of Clinical Investigation*, *112*, 1164–1175. https://doi.org/10.1172/JCI19361

O'Brien, X. M., Heflin, K. E., Lavigne, L. M., Yu, K., Kim, M., Salomon, A. R., & Reichner, J. S. (2012). Lectin site ligation of CR3 induces conformational changes and signaling. *The Journal of Biological Chemistry*, *287*, 3337–3348. https://doi.org/10.1074/jbc.M111.298307

Oda, M., Terao, Y., Sakurai, J., & Nagahama, M. (2015). Membrane-Binding Mechanism of Clostridium perfringens Alpha-Toxin. *Toxins*, *7*, 5268–5275. https://doi.org/10.3390/toxins7124880

Ottico, E., Prinetti, A., Prioni, S., Giannotta, C., Basso, L., Chigorno, V., & Sonnino, S. (2003). Dynamics of membrane lipid domains in neuronal cells differentiated in culture. *Journal of Lipid Research*, *44*, 2142–2151. https://doi.org/10.1194/jlr.M300247-JLR200

Paller, A. S., Arnsmeier, S. L., Chen, J. D., & Woodley, D. T. (1995). Ganglioside GT1b inhibits keratinocyte adhesion and migration on a fibronectin matrix. *The Journal of Investigative Dermatology*, *105*, 237–242. https://doi.org/10.1111/1523-1747.ep12317572

Pan, B., Fromholt, S. E., Hess, E. J., Crawford, T. O., Griffin, J. W., Sheikh, K. A., & Schnaar, R. L. (2005). Myelin-associated glycoprotein and complementary axonal ligands, gangliosides, mediate axon stability in the CNS and PNS: Neuropathology and behavioral deficits in single- and double-null mice. *Experimental Neurology*, *195*, 208–217. https://doi.org/10.1016/j.expneurol.2005.04.017

Pang, H., Le, P. U., & Nabi, I. R. (2004). Ganglioside GM1 levels are a determinant of the extent of caveolae/raft-dependent endocytosis of cholera toxin to the Golgi apparatus. *Journal of Cell Science*, *117*, 1421–1430. https://doi.org/10.1242/jcs.01009

Parasassi, T., De Stasio, G., d'Ubaldo, A., & Gratton, E. (1990). Phase fluctuation in phospholipid membranes revealed by Laurdan fluorescence. *Biophysical Journal*, *57*, 1179–1186. https://doi.org/10.1016/S0006-3495(90)82637-0

Parasassi, T., De Stasio, G., Ravagnan, G., Rusch, R. M., & Gratton, E. (1991). Quantitation of lipid phases in phospholipid vesicles by the generalized polarization of Laurdan fluorescence. *Biophysical Journal*, *60*, 179–189. https://doi.org/10.1016/S0006-3495(91)82041-0

Pfaller, M. A., & Diekema, D. J. (2010). Epidemiology of invasive mycoses in North America. *Critical Reviews in Microbiology*, *36*, 1–53. https://doi.org/10.3109/10408410903241444

Piel, G., Piette, M., Barillaro, V., Castagne, D., Evrard, B., & Delattre, L. (2007). Study of the relationship between lipid binding properties of cyclodextrins and their effect on the integrity of liposomes. *International Journal of Pharmaceutics*, *338*, 35–42. https://doi.org/10.1016/j.ijpharm.2007.01.015

Riethmuller, J., Riehle, A., Grassme, H., & Gulbins, E. (2006). Membrane rafts in host-pathogen interactions. *Biochimica et Biophysica Acta*, *1758*, 2139–2147. https://doi.org/10.1016/j.bbamem.2006.07.017

Rodrigues, M. L., Nakayasu, E. S., Oliveira, D. L., Nimrichter, L., Nosanchuk, J. D., Almeida, I. C., & Casadevall, A. (2008). Extracellular vesicles produced by Cryptococcus neoformans contain protein components associated with virulence. *Eukaryotic Cell*, *7*, 58–67. https://doi.org/10.1128/EC.00370-07

Sanchez, S.A., Tricerri, M.A., Gunther, G. and Gratton, E. (2007) Laurdan generalized polarization: from cuvette to microscope, Formatex, pp. 8.

Schmitz, G., & Orso, E. (2002). CD14 signalling in lipid rafts: New ligands and co-receptors. *Current Opinion in Lipidology*, *13*, 513–521. https://doi.org/10.1097/00041433-200210000-00007

Schnaar, R. L., Fromholt, S. E., Gong, Y., Vyas, A. A., Laroy, W., Wayman, D. M., … Shiekh, K. A. (2002). Immunoglobulin G-class mouse monoclonal antibodies to major brain gangliosides. *Analytical Biochemistry*, *302*, 276–284. https://doi.org/10.1006/abio.2001.5540

Schnaar, R. L., & Needham, L. K. (1994). Thin-layer chromatography of glycosphingolipids. *Methods in Enzymology*, *230*, 371–389. https://doi.org/10.1016/0076-6879(94)30025-9

Sheikh, K. A., Sun, J., Liu, Y., Kawai, H., Crawford, T. O., Proia, R. L., … Schnaar, R. L. (1999). Mice lacking complex gangliosides develop Wallerian degeneration and myelination defects. *Proceedings of the National Academy of Sciences of the United States of America*, *96*, 7532–7537. https://doi.org/10.1073/pnas.96.13.7532

Shi, L., Albuquerque, P. C., Lazar-Molnar, E., Wang, X., Santambrogio, L., Gacser, A., & Nosanchuk, J. D. (2008). A monoclonal antibody to Histoplasma capsulatum alters the intracellular fate of the fungus in

murine macrophages. *Eukaryotic Cell*, *7*, 1109–1117. https://doi.org/10.1128/EC.00036-08

Silvius, J. R. (2003). Role of cholesterol in lipid raft formation: Lessons from lipid model systems. *Biochimica et Biophysica Acta*, *1610*, 174–183. https://doi.org/10.1016/S0005-2736(03)00016-6

Sorgi, C. A., Secatto, A., Fontanari, C., Turato, W. M., Belanger, C., de Medeiros, A. I., … Faccioli, L. H. (2009). Histoplasma capsulatum cell wall {beta}-glucan induces lipid body formation through CD18, TLR2, and dectin-1 receptors: Correlation with leukotriene B4 generation and role in HIV-1 infection. *Journal of Immunology*, *182*, 4025–4035. https://doi.org/10.4049/jimmunol.0801795

Strasser, J. E., Newman, S. L., Ciraolo, G. M., Morris, R. E., Howell, M. L., & Dean, G. E. (1999). Regulation of the macrophage vacuolar ATPase and phagosome-lysosome fusion by Histoplasma capsulatum. *Journal of Immunology*, *162*, 6148–6154.

Sun, J., Shaper, N. L., Itonori, S., Heffer-Lauc, M., Sheikh, K. A., & Schnaar, R. L. (2004). Myelin-associated glycoprotein (Siglec-4) expression is progressively and selectively decreased in the brains of mice lacking complex gangliosides. *Glycobiology*, *14*, 851–857. https://doi.org/10.1093/glycob/cwh107

Superti, F., & Donelli, G. (1991). Gangliosides as binding sites in SA-11 rotavirus infection of LLC-MK2 cells. *The Journal of General Virology*, *72*(Pt 10), 2467–2474. https://doi.org/10.1099/0022-1317-72-10-2467

Takeuchi, O., Hoshino, K., Kawai, T., Sanjo, H., Takada, H., Ogawa, T., … Akira, S. (1999). Differential roles of TLR2 and TLR4 in recognition of gram-negative and gram-positive bacterial cell wall components. *Immunity*, *11*, 443–451. https://doi.org/10.1016/S1074-7613(00)80119-3

Thornton, B. P., Vetvicka, V., Pitman, M., Goldman, R. C., & Ross, G. D. (1996). Analysis of the sugar specificity and molecular location of the beta-glucan-binding lectin site of complement receptor type 3 (CD11b/CD18). *Journal of Immunology*, *156*, 1235–1246.

Triantafilou, M., Miyake, K., Golenbock, D. T., & Triantafilou, K. (2002). Mediators of innate immune recognition of bacteria concentrate in lipid rafts and facilitate lipopolysaccharide-induced cell activation. *Journal of Cell Science*, *115*, 2603–2611.

Triantafilou, M., & Triantafilou, K. (2003). Receptor cluster formation during activation by bacterial products. *Journal of Endotoxin Research*, *9*, 331–335. https://doi.org/10.1177/09680519030090051001

van Echten-Deckert, G. (2000). Sphingolipid extraction and analysis by thin-layer chromatography. *Methods in Enzymology*, *312*, 64–79. https://doi.org/10.1016/S0076-6879(00)12900-3

Viana, N. B., Rocha, M. S., Mesquita, O. N., Mazolli, A., Maia Neto, P. A., & Nussenzveig, H. M. (2007). Towards absolute calibration of optical tweezers. *Physical Review. E, Statistical, Nonlinear, and Soft Matter Physics*, *75*, 021914. https://doi.org/10.1103/PhysRevE.75.021914

Vieira, K.P., e Silva, A. R. D. A., Zollner Lima, Malaguti, C., Vilella, C.A. and de Lima Zollner, R. (2008).Ganglioside GM1 effects on the expression of nerve growth factor (NGF), Trk-A receptor, proinflammatory cytokines and on autoimmune diabetes onset in non-obese diabetic (NOD) mice. *Cytokine 42*, 92–104, https://doi.org/10.1016/j.cyto.2008.01.009

Vieth, J. A., Kim, M. K., Pan, X. Q., Schreiber, A. D., & Worth, R. G. (2010). Differential requirement of lipid rafts for FcgammaRIIA mediated effector activities. *Cellular Immunology*, *265*, 111–119. https://doi.org/10.1016/j.cellimm.2010.07.011

Vyas, K. A., Patel, H. V., Vyas, A. A., & Schnaar, R. L. (2001). Segregation of gangliosides GM1 and GD3 on cell membranes, isolated membrane rafts, and defined supported lipid monolayers. *Biological Chemistry*, *382*, 241–250. https://doi.org/10.1515/BC.2001.031

Watarai, M., Makino, S., Fujii, Y., Okamoto, K., & Shirahata, T. (2002). Modulation of Brucella-induced macropinocytosis by lipid rafts mediates intracellular replication. *Cellular Microbiology*, *4*, 341–355. https://doi.org/10.1046/j.1462-5822.2002.00195.x

Weber, G., & Farris, F. J. (1979). Synthesis and spectral properties of a hydrophobic fluorescent probe: 6-propionyl-2-(dimethylamino)naphthalene. *Biochemistry*, *18*, 3075–3078. https://doi.org/10.1021/bi00581a025

Williamson, J. R., Shanahan, M. O., & Hochmuth, R. M. (1975). The influence of temperature on red cell deformability. *Blood*, *46*, 611–624.

Ywazaki, C. Y., Maza, P. K., Suzuki, E., Takahashi, H. K., & Straus, A. H. (2011). Role of host glycosphingolipids on Paracoccidioides brasiliensis adhesion. *Mycopathologia*, *171*, 325–332. https://doi.org/10.1007/s11046-010-9376-4

Zhou, B., Li, S. C., Laine, R. A., Huang, R. T., & Li, Y. T. (1989). Isolation and characterization of ceramide glycanase from the leech, Macrobdella decora. *Journal of Biological Chemistry*, *264*, 12272–12277.

SUPPORTING INFORMATION

Additional supporting information may be found online in the Supporting Information section at the end of the article.

How to cite this article: Guimarães AJ, de Cerqueira MD, Zamith-Miranda D, et al. Host membrane glycosphingolipids and lipid microdomains facilitate *Histoplasma capsulatum* internalisation by macrophages. *Cellular Microbiology*. 2019;21:e12976. https://doi.org/10.1111/cmi.12976